Agricultural Water Management 317 (2025) 109668

Contents lists available at ScienceDirect

Agricultural Water Management

journal homepage: www.elsevier.com/locate/agwat

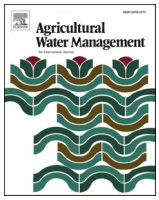

Optimizing wheat yield and water productivity under water scarcity: A modeling approach for irrigation and cultivar selection across different agro-climatic zones of Egypt

Maha L. Elsayed [a,b], Ahmed F. Elkot [c], Tahany Noreldin [d], Benjamin Richard [b,e], Aiming Qi [b], Yasser M. Shabana [f,g], Samir M. Saleh [a], Bruce D.L. Fitt [b], Ahmed M.S. Kheir [h,d,*]

[a] Central Laboratory for Agricultural Climate (CLAC), Agricultural Research Center, Giza 12411, Egypt
[b] Centre for Agriculture, Food and Environmental Management Research, School of Health, Medicine and Life Sciences, University of Hertfordshire, Hatfield, Hertfordshire, AL10 9AB, UK
[c] Wheat Research Department, Field Crops Research Institute, Agricultural Research Center, 12619 Giza, Egypt
[d] Soils, Water and Environment Research Institute, Agricultural Research Center, Giza 12112, Egypt
[e] Agroecology and Environment Research Unit, ISARA, 69007 Lyon, France
[f] Faculty of Agriculture, Mansoura University, Mansoura 35516, Egypt
[g] National Council for Agricultural and Food Research, Academy of Scientific Research and Technology, Cairo 11516, Egypt
[h] Institute for Strategies and Technology Assessment, Julius Kühn Institute (JKI)– Federal Research Centre for Cultivated Plants, Kleinmachnow 14532, Germany

ARTICLE INFO

Keywords:
Deficit irrigation
DSSAT-CERES
CO_2 enrichment
Rising temperature
Resource-use efficiency

ABSTRACT

Egypt, a major wheat importer, grapples with significant food security concerns exacerbated by limited water resources and climate variability. This study investigates strategies to optimize wheat yield and water productivity across Egypt's diverse agro-climatic zones through precise irrigation management and cultivar selection. Using the DSSAT CERES-Wheat model, calibrated with field data from experiments on three wheat cultivars (Sakha94, Shandweel1 and Sids1) under five irrigation treatments across four locations, we evaluated the impact of irrigation frequency and elevated CO_2 levels (390 ppm) on grain yield and water-use efficiency. Results show that frequent irrigation (50 % depletion) increases yield by up to 22 % compared to less frequent irrigation (90 % depletion), particularly for Sakha94, while reduced irrigation enhances water productivity based irrigation (WP_Irrigation), with Shandweel1 and Sids1 achieving 15–20 % higher WP under water-limited conditions. Elevated CO_2 contributes a modest yield increase of approximately 5 % and enhances WP, indicating potential adaptive benefits in future high-CO_2 scenarios. Sensitivity analysis revealed that moderate CO_2 enrichment (+420–440 ppm) combined with + 1°C to + 2°C increases yield and WP by 10–25 %, but higher temperatures (+3°C) shortened growth cycles and reduced benefits, particularly for heat-sensitive cultivars like Sakha94. Linear mixed model analysis further reveals distinct fixed and random effects, underscoring that strategic irrigation management can effectively balance yield maximization and water conservation. These findings highlight the necessity of location-specific irrigation and cultivar strategies to alleviate water scarcity. Future research should prioritize a multi-model ensemble approach to quantify uncertainties, integrate CMIP6 climate projections and explore multi-factor environmental impacts, supporting sustainable wheat production in water-limited regions.

1. Introduction

Food security is intricately tied to the stability and availability of wheat production, as it directly impacts the sustenance of populations (Godfray et al., 2010), particularly in arid and semi-arid regions (Ammar et al., 2024; Kheir et al., 2022a). Ensuring reliable wheat yields under water-scarce conditions is not only vital for meeting domestic demand but also for mitigating the socio-economic risks associated with food shortages (Chiarelli et al., 2022). Water scarcity is one of the most pressing issues faced by arid and semi-arid regions, significantly

* Corresponding author at: Institute for Strategies and Technology Assessment, Julius Kühn Institute (JKI)– Federal Research Centre for Cultivated Plants, Kleinmachnow 14532, Germany.
E-mail addresses: drahmedkheir2015@gmail.com, ahmed.kheir@julius-kuehn.de (A.M.S. Kheir).

https://doi.org/10.1016/j.agwat.2025.109668
Received 4 December 2024; Received in revised form 13 April 2025; Accepted 12 July 2025
Available online 16 July 2025

impacting agricultural productivity (Ingrao et al., 2023; Karimi et al., 2024). In these areas, including Egypt, limited water resources and erratic rainfall pose severe challenges for crop production, particularly for water-intensive crops such as wheat (Abou-Hadid, 2025). Wheat accounts for approximately 30 % of the global grain production and is critical to food security in many regions, including Egypt (Abdalla et al., 2023; Kheir et al., 2025), where it constitutes a significant part of the daily diet (Asseng et al., 2018; Kheir et al., 2024). The reliance on irrigation further exacerbates the stress on water resources in these regions.

Wheat production is a cornerstone of Egypt's food security, yet the country faces significant challenges in meeting its domestic demand, producing only about 50 % of its wheat needs (Gebeltová et al., 2023). With projected increases in temperature and water scarcity, wheat production is expected to decline, exacerbating the already existing food deficit (Kheir et al., 2019). Studies by Kheir et al. (2020a) and Cookson-Hills (2008) highlight that wheat production in Egypt relies heavily on irrigation, as over 95 % of cultivated wheat is grown under irrigated conditions. Moreover, Egypt's limited freshwater resources and high crop water requirements for wheat exacerbate the dependency on irrigation to sustain production levels needed to meet national demand (Abdelhafez et al., 2020). These studies emphasize that irrigation water is the most critical input for wheat production in arid regions, linking water use directly to food security challenges in Egypt. As such, there is an urgent need to explore effective methods to enhance wheat yields while minimizing water use, especially under increasingly arid conditions.

Wheat production in arid and semi-arid regions, such as Egypt, is highly dependent on effective irrigation practices due to limited rainfall and water scarcity (Elkot et al., 2024). Different irrigation regimes can significantly influence grain yield, water productivity, and resource use efficiency. Frequent irrigation, such as maintaining soil moisture depletion at 50 %, has been shown to maximize yield by meeting crop water requirements during critical growth stages (Wu et al., 2024). Conversely, deficit irrigation strategies, which allow for greater soil moisture depletion (e.g., 70–90 %), often improve water productivity by reducing non-productive water losses, though this may come at the cost of reduced yield in sensitive cultivars (Geerts and Raes, 2009). Adopting optimized irrigation schedules that balance yield and water conservation is critical, particularly in regions facing escalating water scarcity. Moreover, combining precise irrigation management with resilient wheat cultivars can mitigate the impacts of water stress, enabling sustainable production under limited water availability. Such strategies are vital for achieving food security in Egypt and other water-scarce regions.

In such water-scarce environments, accurate yield predictions are essential for food security planning and resource allocation (Ding et al., 2021; Kheir et al., 2022b). Predicting wheat yield, especially under varying water availability, enables stakeholders to optimize irrigation schedules, manage resources efficiently, and plan for potential shortfalls in production (Falconnier et al., 2020; Kheir et al., 2021). Yield predictions become even more crucial in the context of increasing climate variability, where water stress conditions are becoming more frequent and severe.

Various crop models, such as DSSAT (Jones et al., 2003) and APSIM (McCown et al., 1996; Pasley et al., 2023), have been developed to simulate crop growth and yield under different environmental and management scenarios, including water stress. These process-based models integrate climate, soil, and crop management to forecast crop performance (Elsayed et al., 2012; Elsayed et al., 2017), allowing for the exploration of various irrigation and planting strategies to improve yield outcomes. The application of these models in arid regions like Egypt is particularly relevant (Solgi et al., 2022; Ziaei and Sepaskhah, 2003), as they can offer the potential measures to mitigate the negative impacts of water stress on wheat yields (Ali et al., 2020).

Despite the advances in process-based modeling, there remain gaps in understanding how different wheat cultivars (Abdelmageed et al., 2019), respond to varying irrigation regimes across diverse agro-climatic zones. Some studies include (Fang et al., 2024; Asseng et al. 2018) demonstrate that cultivar traits, including root architecture, phenological development, and drought tolerance, significantly influence wheat performance under varying irrigation levels. Cultivars with longer grain-filling periods and greater water use efficiency, such as Shandweel1 and Sids1 in this study, tend to perform better under deficit irrigation. Furthermore, Geerts and Raes (2009) highlight how drought-tolerant cultivars can mitigate yield losses in water-scarce conditions, making cultivar selection a vital strategy for balancing yield and water productivity. Current models including DSSAT (Kheir et al., 2020b), APSIM (Kheir et al., 2023), and AquaCrop (Elsadek et al., 2024) have been well-calibrated for certain regions but require further refinement for broader applications under Egypt's specific conditions.

The objectives of this research are to address these gaps by: (i) calibrating and validating the DSSAT model for wheat under different irrigation regimes across Egypt's diverse agro-climatic zones; (ii) deploying the calibrated model to simulate long-term yield and resource use efficiency over the baseline period (1981–2010), incorporating the same irrigation treatments and a single compost application to evaluate its role in enhancing soil fertility and crop performance; and (iii) conducting a comprehensive sensitivity analysis incorporating multiple CO_2 levels (380–460 ppm) and temperature increments (+1°C to +3°C) to evaluate their combined effects on wheat yield, water productivity, and phenology. These objectives aim to provide actionable insights into sustainable irrigation, soil management, and climate adaptation strategies for wheat production in water-scarce regions.

2. Materials and methods

This study utilized a comprehensive approach involving both field experiments and model-based simulations to evaluate the impact of different irrigation regimes on wheat yield under varying agro-climatic conditions in Egypt. Field experiments were conducted across four locations Al-Ismailia Agricultural Research Station (Al-Ismailia), Nubaria Agricultural Research Station (Al-Behera), Sids Agricultural Research Station (Bani Suef) and Al Mataenah Agricultural Research Station (Luxor) over two cropping seasons. These experiments tested three wheat cultivars (Sakha94, Sids1 and Shandweel1) under five irrigation treatments. Data on environmental factors, including temperature, humidity, wind speed, and evapotranspiration, were collected throughout the growing seasons to inform model inputs. The CERES-Wheat module within the DSSAT framework is a process-based model which simulates plant growth and development on a daily time-step. It was used for the simulation and calibrated using genetic coefficients specific to the wheat cultivars tested. Calibration of the model was done to align the simulated values with observed values in the field experiments for anthesis date, maturity date, grain yield and biomass yield.

2.1. Field experiment and soil characteristics

A field experiment was conducted in four distinct locations across Egypt, representing diverse agro-climatic conditions (S. Fig. 1). These locations vary significantly in latitude, longitude, altitude, soil texture type, and soil available water content (SAWC) at field capacity, which provided a comprehensive range of environmental conditions for the study. The experimental sites were used to test three high-yielding spring wheat cultivars (Sakha94, Sids1 and Shandweel1) over two cropping seasons: 2019/2020 and 2020/2021 at Al-Behera and Bani Suef, and 2020/2021 and 2021/2022 at Al-Ismailia and Luxor, respectively. These experiments were crucial for evaluating the performance of the wheat cultivars under different irrigation regimes and weather and soil conditions. Final aboveground biomass was measured by harvesting plants from a representative 2.8 m^2 plot within each experimental plot. The harvested biomass was dried in an oven at 70°C until a constant weight was achieved, and the dry weight was recorded for further using in model calibrations.

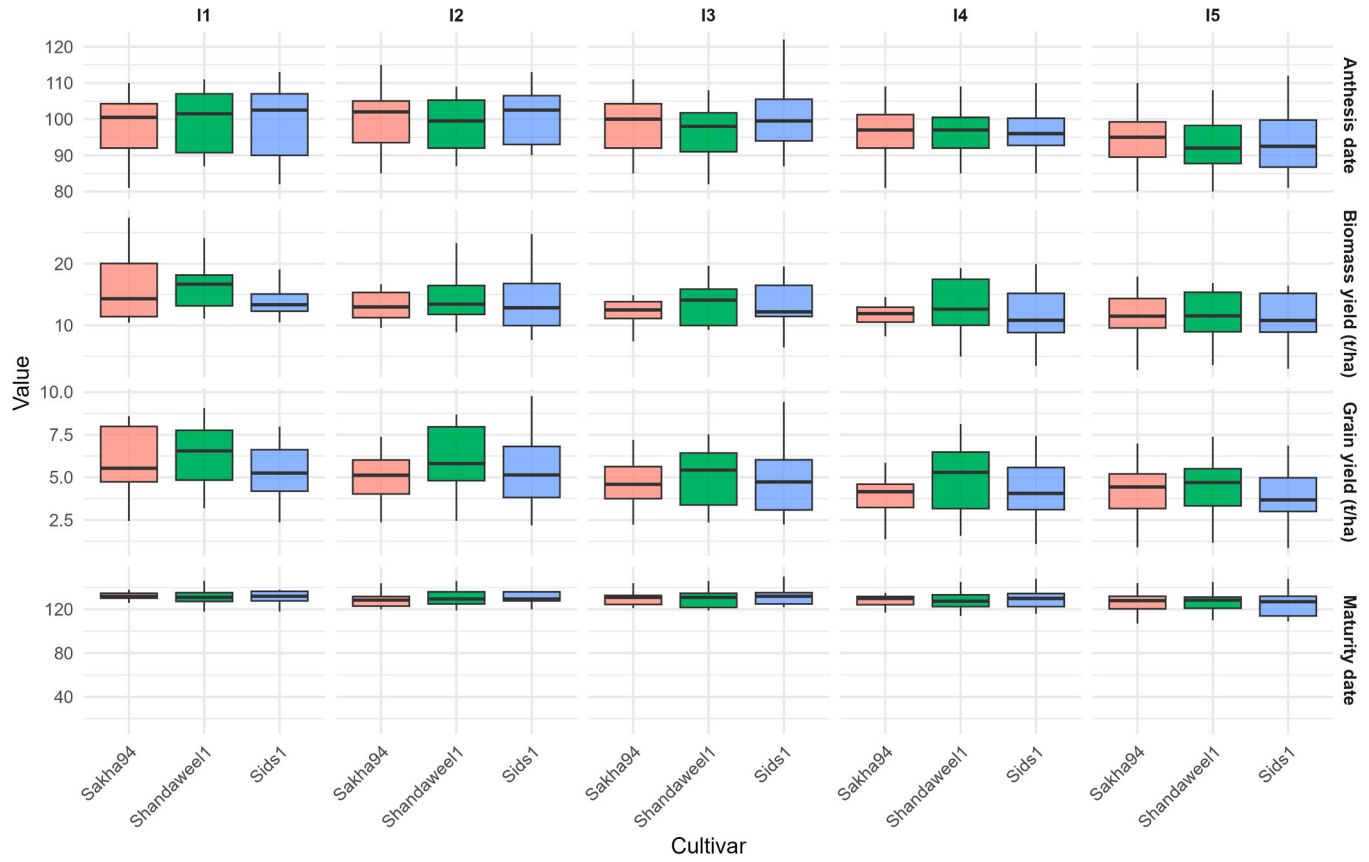

Fig. 1. Distribution of observed anthesis date, maturity date, grain yield, and biomass yield across three wheat cultivars (Sakha94, Shandweel1, Sids1) and five irrigation treatments (I1–I5). Each boxplot summarizes three replicates per treatment, over two growing seasons. This figure illustrates the variability in phenological development and productivity used for model calibration and evaluation.

2.2. Environmental and soil conditions of the experimental sites

Mean maximum and minimum air temperature (°C), global radiation (MJ), rainfall, (mm), relative humidity, wind speed, and potential evapotranspiration (ET_o) were obtained from the central laboratory for agriculture climate (CLAC) and recorded daily from sowing date to end of May in the next year were measured in each cropping season at four locations (Table 2). The predominant soil analysis including soil physical and chemical properties in the DSSAT format (Supplementary Table 1).

2.3. Treatments

The experiments employed five irrigation treatments across three wheat cultivars (Sakha94, Sids1 and Shandweel1). Initial irrigation following dry sowing was applied to support seedling emergence and ensure crop establishment. Supplementary Table 1 details the five irrigation treatments, with application frequencies progressively reduced from six applications in Treatment 1 (I1) to two applications in Treatment 5 (I5), each administered at specific intervals post-sowing.

2.4. Calibrations and evaluations of DSSAT CERES wheat model

Calibrating the DSSAT CERES-Wheat model required ensuring that the phenological development functions accurately reflected agronomic relevance in response to crop management practices and environmental conditions. The DSSAT-CERES-Wheat model was calibrated using field data from the first growing season under non-stress conditions and subsequently evaluated using observations from the second growing season, following the calibration protocol outlined by Janssen and Heuberger (1995). Calibration was performed by adjusting cultivar-specific genetic coefficients to align simulated outputs with observed phenological and yield traits. The process began with the calibration of phenological development (anthesis and maturity), followed by calibration of grain yield and biomass for the three studied cultivars. The genetic coefficients were estimated based on observed phenology and yield components (Table 3), and are essential for capturing the distinct phenological patterns and productivity potential

Table 1
Experimental locations with latitude (°), longitude (°), altitude (m), soil texture type soil available water content (SAWC) at field capacity and sowing date.

Location	Latitude	Longitude	Altitude	Soil type	SAWC	Sowing date
Al-Behera	30.9	29.87	54	Loamy Sand	12 %	05-Dec–2019
				Loamy Sand	13 %	25-Nov–2020
Al-Ismailia	30.52	31.96	5	Sandy Soil	12 %	13-Dec–2020
				Sandy Soil	12 %	21-Nov–2021
Bani Suef	28.9	30.95	18	Clay	19 %	01-Dec–2019
				Clay	18 %	25-Nov–2020
Luxor	25.42	32.53	82	Clay loam	18 %	25-Nov–2020
				Clay loam	18 %	27-Nov–2021

Table 2
Mean maximum (Tmax), minimum (Tmin), average (Tave) air temperature, average relative humidity (RH), wind speed (WS), total rainfall (R), global radiation (Rad) and potential evapotranspiration (ET_o) from sowing date to end of May in next year in each cropping season at four locations.

Location	Sowing date	Tmax (°C)	Tmin (°C)	Tave (°C)	Rad (MJ)	R (mm)	RH (%)	WS ($m\ s^{-1}$)	ET_o (mm)
Al-Behera	05-Dec−2019	22.1	12.7	17.4	3535.8	288.0	68.8	3.5	700.6
	25-Nov−2020	23.6	13.3	18.4	3717.9	264.1	65.7	3.1	757.3
Al-Ismailia	13-Dec−2020	27.0	11.5	19.3	3351.7	81.6	57.5	2.5	706.9
	21-Nov−2021	24.9	10.7	17.8	3288.9	22.0	56.4	2.7	670.6
Bani Suef	01-Dec−2019	24.4	10.2	17.3	3731.0	100.8	54.4	2.9	746.3
	25-Nov−2020	26.7	11.4	19.1	3910.1	29.9	45.7	2.9	817.2
Luxor	25-Nov−2020	29.8	12.4	21.1	4169.6	0.8	30.8	2.8	916.4
	27-Nov−2021	28.0	11.6	19.8	3915.9	5.6	33.8	3.0	836.3

Table 3
Genetic coefficients under CERES-Wheat used for model calibration of Sakha94, Sids1 and Shandaweel1 cultivars.

Genetic Co-efficient	Sakha94	Sids1	Shandweel1
P1V Days, optimum vernalizing temperature, required for vernalization	52.68	27.72	23.55
P1D Photoperiod response (% reduction in rate/10 h drop in pp)	46.66	48.55	40.11
P5 Grain filling (excluding lag) phase duration (°C. d)	382.7	519.9	460.2
G1 Kernel number per unit canopy weight at anthesis (#/g)	14.33	37.60	29.12
G2 Standard kernel weight under optimum conditions (mg)	44.21	18.12	23.75
G3 Standard, non-stressed mature tiller wt (incl grain) (g dwt)	0.85	4.74	3.26
PHINT Interval between successive leaf tip appearances (°C. d)	100.0	100.0	100.0

of each cultivar under varying environmental conditions and irrigation treatments. By adjusting species, ecotype, and cultivar-specific coefficients, the DSSAT model enables the simulation of phenological and growth responses across multiple crop species and cultivars. In this study, we applied the Generalized Likelihood Uncertainty Estimation (GLUE) method (Jones et al., 2011), which optimizes cultivar coefficients by comparing actual and simulated yield values using Bayesian estimation based on Gaussian likelihood functions and Monte Carlo sampling. GLUE inputs are incorporated into the model through File-A (Jones et al., 2011). File A in DSSAT, also known as the "Experiment Management" file, is a key input file that defines the management practices, experimental design, and specific treatments applied during a simulation. It provides the framework for running simulations by linking environmental conditions with management practices. Table 3 presents the genetic coefficients calibrated using this approach.

GLUE method was used to quantify parameter uncertainty and improve the reliability of wheat performance predictions under diverse environmental and management conditions. A total of 4000 simulations were run using cultivar-specific data within the DSSAT system. GLUE identifies acceptable parameter sets based on a likelihood function, generating posterior distributions that reflect uncertainty (Han et al., 2014; Li et al., 2010). The optimized parameters were then analyzed and incorporated into the DSSAT cultivar file, effectively reducing uncertainty and enhancing model robustness.

For evaluation, simulated values for yield, final biomass and phenology were compared with observed data under all irrigation treatments to assess model accuracy. The evaluation used statistical metrics, including the coefficient of determination (R^2) (Cheng et al., 2014), Root Mean Square Deviation (RMSD) (Pathria and Beale, 2011), and the index of agreement (d-index) (İldan, 2010; Jacovides and Kontoyiannis, 1995).

2.5. Application of DSSAT for long term simulation over the historical period

Following calibration and evaluation, the model was deployed for long-term simulations over the baseline period (1981–2010) using different automatic deficit irrigation based on soil moisture depletion. In the DSSAT model, automatic irrigation scheduling based on soil moisture depletion is a key feature for optimizing water use and enhancing crop productivity under variable water conditions. This approach allows irrigation to be triggered at specific depletion levels of soil available water, ensuring that crops receive water just before reaching critical moisture deficits. Here, irrigation was scheduled at soil moisture depletion levels of 50 %, 60 %, 70 %, 80 % and 90 % of the available water holding capacity. This percentage represents the proportion of the soil's moisture reserve that has been used by the crop since the last irrigation or rainfall event. This method was controlled by changing the code ITRHL (Threshold for Irrigation Trigger) with 50, 40, 30, 20 and 10 to ensure soil moisture depletion levels of 50 %, 60 %, 70 %, 80 %, and 90 % of the available water holding capacity respectively. When the depletion threshold is reached, the DSSAT model calculates the required irrigation quota to restore soil moisture to field capacity, which is achieved by setting the ITRHU (Irrigation Threshold Refill to Field Capacity) parameter. This quota is determined by the amount of water needed to replenish the soil profile from the current depletion level up to field capacity, ensuring optimal moisture availability for root uptake without oversaturating the soil. By utilizing this threshold-based approach, DSSAT enables precise irrigation management, reducing water wastage and stress to crops, which is particularly beneficial in regions with limited water resources or erratic rainfall patterns. Additionally, simulations incorporated two CO_2 levels (380 ppm and 390 ppm) and a compost application to assess optimal management practices for enhancing wheat yield and water productivity. AgMERRA Climate Forcing Dataset for Agricultural Modeling was used for the long-term simulations. It contains the AgMIP climate forcing dataset based on the NASA Modern-Era Restrospective Analysis for Research and Applications (MERRA). AgMERRA corrects to gridded temperature and precipitation, incorporates satellite precipitation, and replaces solar radiation with NASA/GEWEX SRB to cover the 1980–2010 period (Ruane et al., 2015). We selected the period 1981–2010 for long-term simulations because high-quality daily weather data from the AgMERRA dataset are only available for this timeframe. The AgMERRA dataset provides corrected historical climate data tailored for agricultural modeling, ensuring consistency and accuracy in simulating wheat growth under realistic environmental conditions. Water productivity was calculated as the ratio of grain yield (kg/ha) to actual evapotranspiration (mm), as simulated by the DSSAT model, to evaluate crop water use efficiency.

2.6. Sensitvity analysis

To assess the combined impacts of elevated atmospheric carbon dioxide (CO_2) levels and temperature increases on wheat yield, water

productivity, and phenology, we conducted a sensitivity analysis using the DSSAT CERES-Wheat model. This analysis included three temperature increments (+1°C, +2°C, and +3°C) and five CO_2 concentrations (380 ppm, 400 ppm, 420 ppm, 440 ppm, and 460 ppm), resulting in 15 temperature × CO_2 combinations. These scenarios were applied to three wheat cultivars (Sakha94, Shandweel1, and Sids1) under five irrigation treatments (50 %–90 % soil moisture depletion) across four diverse agro-climatic zones in Egypt (Al-Ismailia, Luxor, Al-Behera, and Bani Suef) over a 30-year baseline period (1981–2010). Climate data were obtained from the AgMERRA dataset to ensure consistency with historical weather patterns. Outputs such as grain yield, water productivity, evapotranspiration, and growth cycle duration were analyzed to evaluate cultivar-specific and irrigation-specific responses to future climate conditions. This analysis provided key insights into the interactive effects of CO_2 and temperature on wheat productivity, highlighting trade-offs between yield optimization and water conservation under projected climate scenarios.

2.7. Statistical analysis

All statistical analyses were conducted using R software (R Core Team, 2024) to evaluate model accuracy and explore relationships among variables. In the analysis, a comprehensive statistical approach was used to evaluate the effects of different cultivars and irrigation treatments on wheat yield, biomass and phenological development under water-limited conditions. Linear mixed models were employed to examine both fixed and random effects, specifically analyzing the influence of cultivar (Sakha94 and Sids1) and irrigation treatments and the model's performance was assessed using several key model fitness performance metrics. The statistical indicators R^2, RMSD and d-index were calculated using custom formulas and the *Metrics* package, allowing the evaluation of the goodness of fit between observed and simulated values for yield, biomass and phenology. Additionally, Principal Component Analysis (PCA) was conducted using the *FactoMineR* and *factoextra* packages to reveal the variance structure and relationships among environmental and yield variables, facilitating dimensionality reduction and pattern recognition across irrigation treatments and cultivars. Boxplots generated with *ggplot2* provided visual insights into yield and biomass distribution across treatments, while pairwise scatter plots (pairplots) created with the *GGally* package allowed for exploration of correlations and interactions among key agronomic variables like yield, biomass, and phenology. This multifaceted analysis framework, supported by these R packages, offered robust insights into model performance, treatment effects, and variable relationships, thereby identifying optimal irrigation management practices for wheat under different soil moisture conditions, as illustrated by the fixed and random effects shown in the linear mixed model outputs.

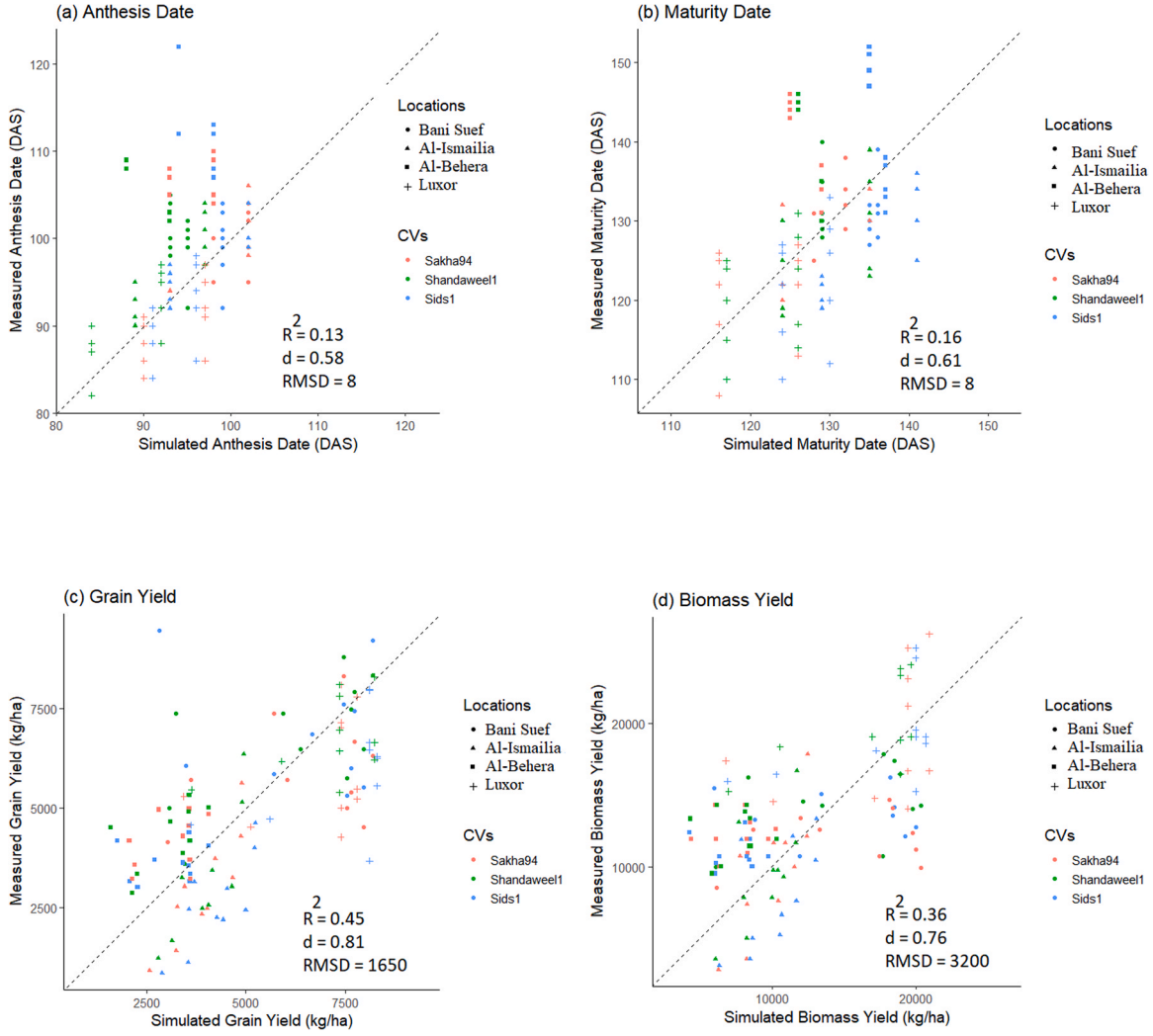

Fig. 2. Scattered comparison between measured and simulated (a) anthesis date, (b) maturity date, (c) grain yield and (d) biomass yield in four locations for three different wheat cultivars.

3. Results

3.1. Calibration and evaluation of CERES-wheat model

To better understand the variability in the observed field data used for model calibration and evaluation, boxplots were generated for anthesis date, maturity date, grain yield, and biomass yield across the three cultivars (Sakha94, Shandweel1, and Sids1) under five irrigation treatments (I1–I5) (Fig. 1). The distributions reveal notable differences among cultivars and treatments, particularly under water stress (I4 and I5), where both yield and phenological development showed higher variability. Sakha94 generally exhibited earlier phenological stages and higher grain weight, while Shandweel1 and Sids1 produced higher biomass under well-watered conditions. These patterns illustrate the underlying data structure used in calibration and highlight the diverse cultivar responses that contributed to variability in model performance. The calibration and evaluation of the DSSAT CERES-Wheat model are presented in Fig. 2, which provides scatter plots comparing measured versus simulated values for anthesis date, maturity date, grain yield and biomass yield across four locations (Bani Suef, Al-Ismailia, Al-Behera and Luxor) and three wheat cultivars (Sakha94, Shandweel1 and Sids1). The model's performance (goodness of fit) in capturing phenological development and yield outcomes is assessed through metrics including R^2, d, and RMSD, which together provide a comprehensive evaluation of the model's accuracy. For anthesis date (Fig. 2a), the model showed a moderate level of agreement with observed values, with an R^2 value of 0.13, a d-index of 0.58, and an RMSD of 8 days. These values indicate that the model could explain some variability in anthesis timing across the different locations and cultivars, though its predictive precision is limited. The observed discrepancies suggest that while the model accounts for general phenological trends, specific environmental and genetic interactions affecting anthesis timing may not be fully explained. Variability in temperature and photoperiod sensitivity across cultivars and regions probably contributes to these differences, highlighting areas where the model could be refined for enhanced phenological accuracy.

The model demonstrated slightly improved performance for maturity date (Fig. 2b), as indicated by an R^2 of 0.16, a d-index of 0.61 and RMSD of 8 days. While the R^2 values (0.13 for anthesis and 0.16 for maturity) indicate limited explanatory power for variability in phenological dates, the d-index provides a complementary perspective on model performance. The d-index values (0.58 for anthesis and 0.61 for maturity) suggest moderate agreement between observed and simulated values, capturing the overall trends in phenological development across locations and cultivars. The d-index, or Willmott's index of agreement, ranges from 0 to 1, where values closer to 1 indicate better agreement between observed and simulated values. Values around 0.6, as reported in this study, indicate that the model captures the general patterns of anthesis and maturity timing but could be improved further for precision. These values are comparable to other studies that used process-based crop models in diverse environments and reflect the inherent challenges of simulating phenological events influenced by complex environmental and genetic interactions (e.g., temperature fluctuations, photoperiod sensitivity). This suggests that the model captures the general trend in wheat maturity timing reasonably well. However, similar to anthesis date, some deviations from the observed values are apparent, which may reflect site-specific climate effects or cultivar responses not fully integrated into the model's parameters. The maturity date results underscore the model's ability to simulate general phenological development, albeit with some limitations in precision, particularly across different environmental conditions and management practices.

Grain yield predictions (Fig. 2c) showed moderate accuracy with an R^2 value of 0.45, a d-index of 0.81 and RMSD of 1650 kg/ha, suggesting that the model is relatively effective at explaining yield variability across different irrigation treatments and cultivars. The higher d-index value reflects a stronger agreement between observed and simulated yields, indicating that the model adequately represents the influence of irrigation and cultivar differences on yield potential. Nevertheless, certain points deviate from the 1:1 line, suggesting instances where the model either overestimates or underestimates actual grain yield. These deviations could be attributed to unaccounted factors such as nutrient availability, pest and disease pressures or microclimatic variations that affect yield.

In terms of aboveground biomass yield (Fig. 2d), the model showed the highest level of agreement among the parameters evaluated, with an R^2 of 0.36, a d-index of 0.76, and an RMSD of 3200 kg/ha. This indicates that the model explains the general trend in biomass production across different environments and cultivars, although variability remains that the model does not fully explain. The relatively good agreement in biomass prediction suggests that the model is well-suited for simulating overall growth responses under the given irrigation treatments. The deviations, however, point to potential influences of local environmental conditions or unmodelled management practices that may affect biomass accumulation rates differently in each location.

Overall, the model's calibration and evaluation results reveal that it provides reasonable predictions for phenological stages and yield components, with greater accuracy for grain and biomass yields than for anthesis and maturity dates. The observed discrepancies, particularly in phenology, suggest potential areas for model refinement, especially in incorporating location- and cultivar-specific responses to environmental and management factors. Despite these limitations, the model demonstrates utility in simulating wheat performance under diverse irrigation regimes, supporting its use for exploring optimal management practices under varying agro-climatic conditions. The results provide a foundation for further model adjustments to enhance predictive accuracy, especially for phenological events sensitive to specific environmental cues.

Figs. 3, 4, and 5 provide a comprehensive analysis of the model's predictive performance across various factors, including irrigation treatment, location and wheat cultivar, for anthesis date, maturity date, grain yield, and biomass yield. These figures illustrate the model's capability in explaining both phenological and yield outcomes under diverse conditions, offering insights into its robustness and areas for improvement.

In Fig. 3, the model's predictions for anthesis date, maturity date, grain yield, and biomass yield are compared with observed values across five distinct irrigation treatments. The scatter plots reveal that the model generally aligns well with observed trends, with varying levels of accuracy across the phenological stages and yield parameters. Anthesis and maturity dates display moderate alignment with observed values, though some variability remains, particularly under extreme irrigation levels. For grain yield and biomass yield, the model shows closer agreement with observed values under moderate irrigation treatments, suggesting that the model explains the response of yield to water availability but may require adjustments for extreme water stress or excess scenarios. The overall patterns indicate the model's sensitivity to irrigation variations and its relative strength in yield prediction under moderate irrigation.

Fig. 4 represents a paired comparison of model performance across four diverse locations: Bani Suef, Al-Ismailia, Al-Behera, and Luxor. The model's ability to explain phenological and yield outcomes in varied environmental conditions is shown in these plots. Anthesis date and maturity date predictions exhibit reasonable agreement with observed values, with the strongest correlations in Al-Behera and Luxor, where environmental conditions align closely with the model's calibration parameters. Grain yield and biomass yield predictions indicate a strong alignment in Bani Suef and Al-Ismailia, suggesting that the model is well-suited to simulate yield in regions with similar environmental characteristics. However, some discrepancies are noted in extreme climates, such as the higher temperatures in Luxor, where biomass yield deviations suggest a potential need for location-specific calibration to enhance predictive accuracy. Overall, Fig. 4 highlights the model's

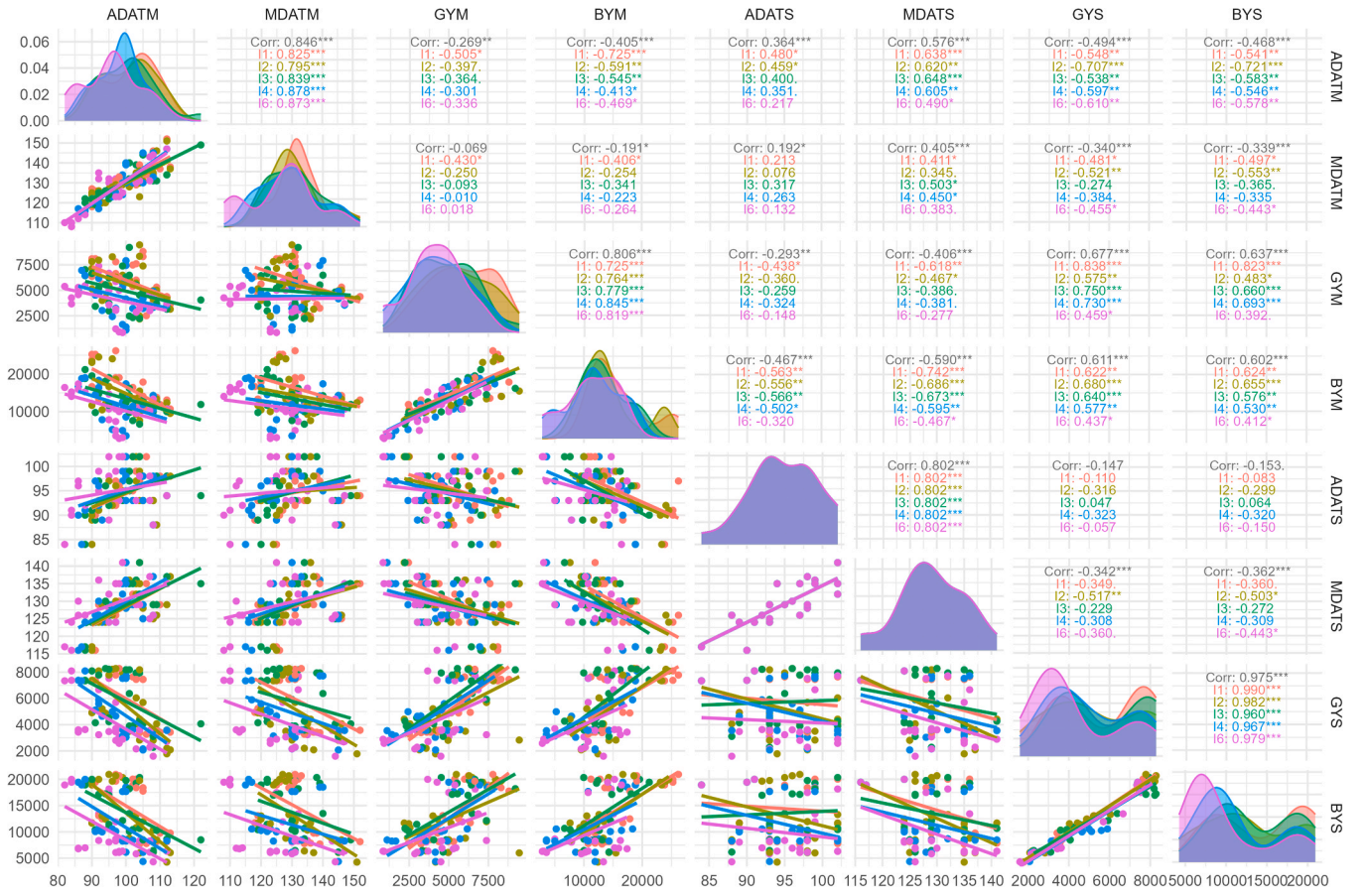

Fig. 3. Paired comparison between measured and simulated values for anthesis date (ADATM and ADATS), maturity date (MDATM and MDATS), grain yield (GYM, and GYS), and biomass yield (BYM and BYS) across five irrigation treatments in the DSSAT CERES-Wheat model. The irrigation treatments range from frequent to limited applications, reflecting varying water availability conditions. Each point represents a unique combination of treatment, location, and cultivar. The model's predictive accuracy under different irrigation levels highlights its sensitivity to water availability and its capacity to simulate phenological and yield responses under both water-stressed and well-watered conditions. Discrepancies observed under extreme irrigation treatments suggest potential areas for model refinement.

robustness in explaining phenological and yield trends across a range of agro-climatic zones, with the potential for refinement in extreme environmental conditions.

In Fig. 5, the model's predictive accuracy is assessed across three wheat cultivars: Sakha94, Shandweel1, and Sids1. This figure reveals the model's capacity to simulate cultivar-specific phenological and yield characteristics. The anthesis date and maturity date demonstrate a good fit with observed values for all cultivars, though Sakha94 shows slightly more variation, possibly due to its unique phenological response to environmental cues. For grain yield and biomass yield, Shandweel1 exhibits the closest alignment between observed and simulated values, indicating that the model parameters align well with this cultivar's growth characteristics. In contrast, slight deviations for Sakha94 and Sids1 suggest that adjustments to cultivar-specific coefficients could further improve predictive accuracy. These findings emphasize the model's general adaptability across cultivars while indicating opportunities to enhance calibration for each variety.

Collectively, Fig. 3&4 and 5 demonstrate the DSSAT CERES-Wheat model's ability to predict key phenological stages and yield parameters under various irrigation treatments, environmental conditions, and cultivar types. While the model shows strong performance under moderate irrigation and typical environmental conditions, minor discrepancies in extreme scenarios or specific cultivars suggest potential areas for further refinement. These results confirm the model's utility in simulating wheat performance across diverse management practices and environmental settings, with targeted adjustments capable of enhancing its overall predictive reliability.

Fig. 6 presents a Principal Component Analysis (PCA) of key phenological and yield traits across three wheat cultivars (Sakha94, Shandweel1 and Sids1) and five irrigation treatments (I1–I5). The PCA results highlight the relationships and variability of these traits under different genetic and management conditions, offering insights into the primary factors influencing wheat performance.

In Fig. 6a, the PCA is grouped by cultivar, displaying each cultivar's distinctive influence on the distribution of phenological and yield traits. The two principal components (PC1 and PC2) together explain a substantial portion (70 %) of the variability among the traits. Traits such as anthesis date (ADATS), maturity date (MDATS), grain yield (GYM), and biomass yield (BYM) show specific loadings along the principal components, reflecting the cultivars' different genetic responses. Shandweel1, represented by green triangles, shows a broader spread along PC1 and PC2, suggesting higher variability in response to environmental conditions and management practices. Sakha94 (red circles) and Sids1 (blue squares) cluster more closely around the origin, indicating more consistent responses. The vector directions for each trait imply that maturity and anthesis dates are closely associated with PC1, while yield-related traits, such as grain yield and biomass yield, show strong associations with PC2.

Fig. 6b illustrates the PCA with grouping based on irrigation treatments (I1-I5), where each irrigation treatment influences the spread and orientation of the phenological and yield traits. Treatments I1 and I5, represented by red circles and pink crosses, respectively, display broader dispersions along PC1, indicating that extreme irrigation levels (both high and low) contribute to greater variability in trait responses.

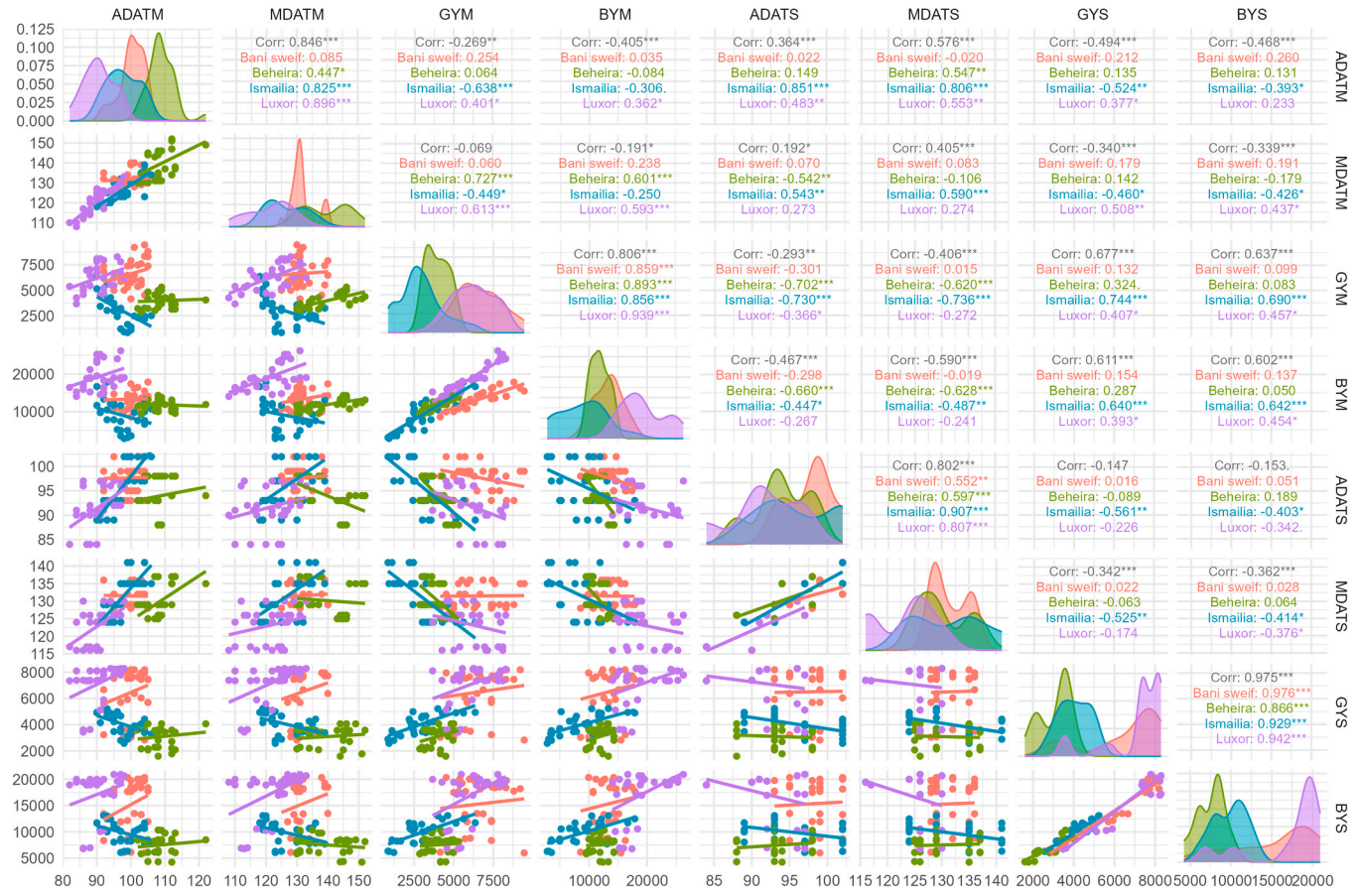

Fig. 4. Paired comparison between measured and simulated values for anthesis date (ADATM and ADATS), maturity date (MDATM and MDATS), grain yield (GYM, and GYS), and biomass yield (BYM and BYS) across four locations: Bani Suef, Al-Ismailia, Al-Behera, and Luxor. Each point corresponds to a unique location, cultivar, and irrigation treatment combination. This figure illustrates the model's capability to capture the effects of different agro-climatic conditions on phenology and yield components. Strong alignment in moderate climates, such as those in Bani Suef and Al-Ismailia, demonstrates the model's reliability, while deviations in Luxor, where extreme temperatures prevail, suggest a need for location-specific adjustments. The figure emphasizes the model's adaptability to diverse environmental conditions while also highlighting areas for further improvement under extreme climate conditions.

Conversely, moderate irrigation treatments (I2, I3 and I4) are positioned closer to the center, reflecting less variability and a more stable response pattern for the measured traits. Traits like grain yield, and biomass yield are strongly aligned with PC2, emphasizing that these yield components are more responsive to changes in water availability than phenological traits. The PCA vectors suggest that yield traits tend to increase with moderate irrigation, as reflected by the central clustering of treatments I2 to I4. Overall, the PCA in Fig. 6 highlights the complex interplay between genetic and irrigation influences on wheat phenology and yield. Cultivar-specific grouping reveals inherent genetic variability, while irrigation-based grouping emphasizes water availability's critical role in determining yield outcomes. These results underscore the need for tailored management practices that consider both genetic and environmental factors to optimize wheat productivity under varying irrigation regimes.

3.2. *Long term simulation of yield, ET and water productivity*

Fig. 7 presents the results of long-term simulations (1980–2010) on the grain yield (GY) of three wheat cultivars (Sakha94, Shandweel1 and Sids1) in Egypt under varying irrigation treatments, CO_2 concentrations and locations. This figure shows that grain yield is significantly affected by irrigation level, CO_2 concentration and agro-climatic conditions, with each subplot representing a unique combination of cultivar, CO_2 level (380 ppm or 390 ppm) and location (Al-Ismailia, Luxor, Al-Behera and Bani Suef). Across all cultivars and locations, there is a clear trend of increased grain yield with higher levels of irrigation (lower depletion rate), indicating that more frequent irrigation positively influences yield (S. Table 3). The results demonstrate substantial variability in grain yield responses across locations, suggesting that environmental conditions play a crucial role in how each cultivar performs under specific irrigation regimes. For example, higher yields are generally observed in Al-Behera and Luxor compared to Al-Ismailia and Bani Suef, which may be attributed to differences in soil type, temperature, and other site-specific factors. The two CO_2 levels further highlight the potential impact of elevated CO_2 on wheat yield, with slightly higher yields observed at 390 ppm in most cases, suggesting that increased CO_2 may enhance photosynthesis and crop productivity, albeit with varying effects across cultivars and locations. Each cultivar exhibits a distinct response pattern to the irrigation treatments. Sakha94 generally shows higher yield responses to increased irrigation, especially under elevated CO_2 conditions, while Shandweel1 and Sids1 display more variable yield patterns across different locations. These differences underline the importance of selecting suitable cultivars based on local environmental conditions and available water resources (Abdelmageed et al., 2019), as each cultivar's yield response may be optimized with targeted irrigation strategies. Statistical significance indicators between irrigation treatments reveal that, in most cases, yield differences between treatments are highly significant ($p < 0.001$), emphasizing the strong influence of irrigation frequency on wheat productivity. The statistical comparisons indicate that while I1 (50 % depletion) generally produces the highest yields across cultivars and CO_2 levels, moderate irrigation levels like I2

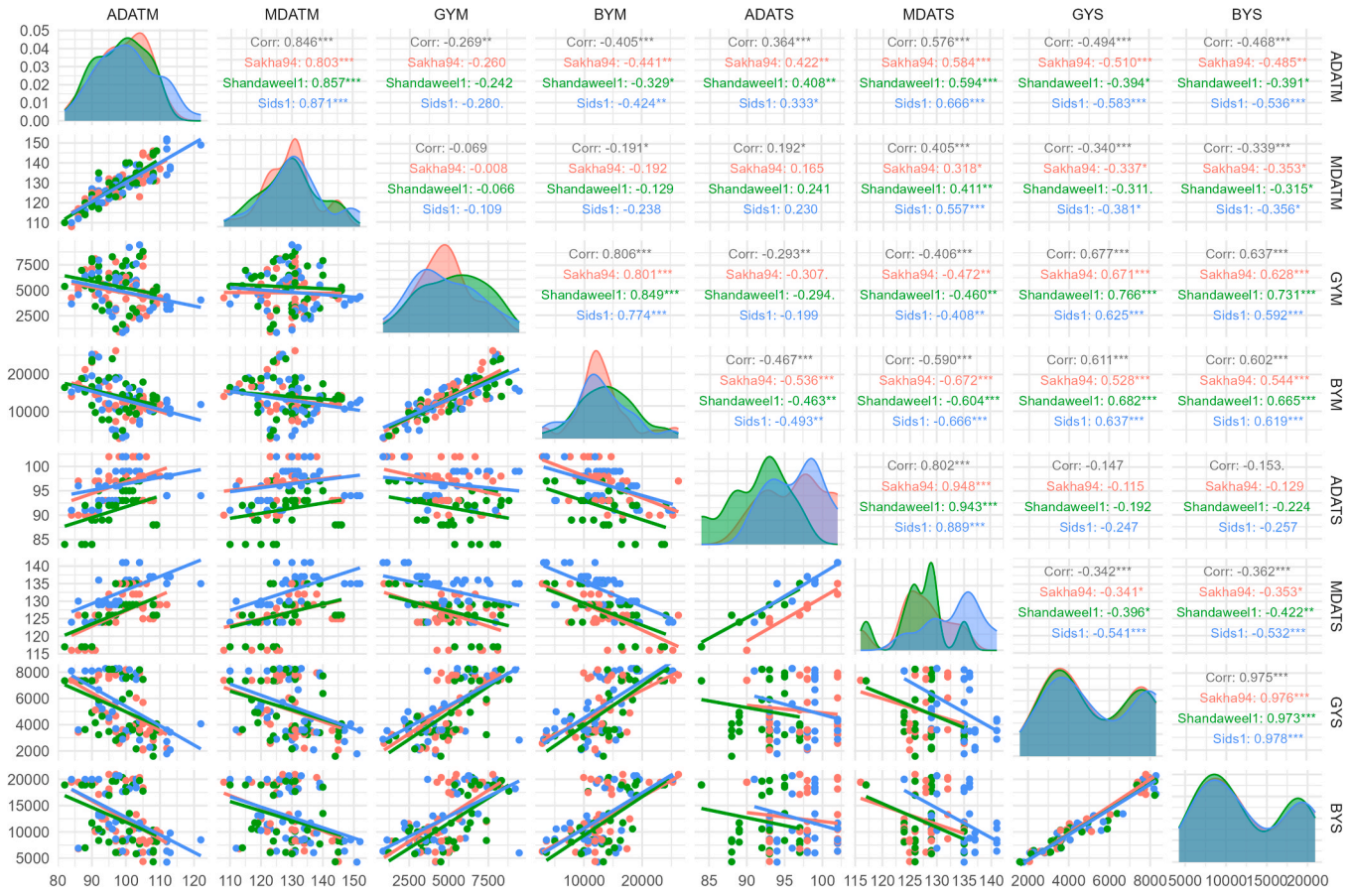

Fig. 5. Paired comparison between measured and simulated values for anthesis date (ADATM and ADATS), maturity date (MDATM and MDATS), grain yield (GYM and GYS), and biomass yield (BYM, and BYS) across three wheat cultivars: Sakha94, Shandweel1, and Sids1. Each data point represents a specific cultivar in combination with different locations and irrigation treatments. The figure demonstrates the model's accuracy in predicting cultivar-specific growth stages and yield outcomes, with Shandweel1 showing the closest alignment with observed values. Variations in Sakha94 and Sids1 indicate possible areas for cultivar-specific calibration to improve model accuracy. This figure highlights the model's flexibility in accommodating different wheat genotypes, as well as its potential for enhanced performance with further calibration for each variety.

and I3 also perform well, particularly in locations with higher yield potential, such as Al-Behera and Luxor. These results suggest that moderate irrigation regimes may achieve a balance between yield optimization and water conservation, which is critical in water-scarce regions like Egypt. Overall, Fig. 7 emphasizes the need for location- and cultivar-specific irrigation strategies to maximize grain yield under variable CO_2 scenarios. By analyzing the combined effects of irrigation treatment, CO_2 level and environmental conditions, this study provides valuable insights into how different wheat cultivars can be managed to optimize yield in Egypt's diverse agro-climatic zones. This evidence supports the development of sustainable irrigation practices that consider both cultivar adaptability and the potential benefits of elevated CO_2, enabling more efficient use of limited water resources while maintaining high crop productivity.

Supplementary Figure 2 shows the impact of different irrigation treatment, CO_2 level, and location on the actual evapotranspiration (ET) of three wheat cultivars (Sakha94, Shandweel1 and Sids1) in Egypt. The results reveal that ET varies significantly across irrigation treatments, CO_2 concentrations, and locations, with irrigation treatments (I1 to I5) representing irrigation at 50 %, 60 %, 70 %, 80 % and 90 % depletion of soil available water, respectively. Across all combinations of cultivars, CO_2 levels (380 ppm and 390 ppm) and locations (Al-Ismailia, Luxor, Al-Behera and Bani Suef), ET consistently decreases with reduced irrigation frequency, as indicated by the lower ET values under I4 and I5 treatments. This trend highlights the direct influence of irrigation on ET, where more frequent watering increases water availability for crop uptake and transpiration. Significant differences in ET between treatments, indicated by p-values (< 0.001), suggest that irrigation scheduling notably impacts water use across locations. Generally, higher ET is observed in Al-Behera and Luxor compared to Al-Ismailia and Bani Suef, probably due to variations in environmental conditions such as temperature, humidity, and soil characteristics. The elevated CO_2 level (390 ppm) slightly reduces ET across all treatments and locations, which aligns with findings suggesting that increased CO_2 can enhance water-use efficiency by partially reducing stomatal conductance. Cultivars display unique responses to the irrigation treatments, with Sakha94 generally showing higher ET compared to Shandweel1 and Sids1 across all locations, particularly under higher irrigation frequencies (I1 and I2). This cultivar-specific ET response underlines the importance of selecting cultivars with suitable water-use characteristics for different agro-climatic conditions, as Sakha94 may require more frequent irrigation to sustain optimal growth and yield, while Shandweel1 and Sids1 may perform better under moderate irrigation regimes.

S. Fig. 3 displays the amount of irrigation applied (mm) under different treatments, CO_2 levels and locations for three wheat cultivars (Sakha94, Shandweel1 and Sids1) in Egypt. Across all combinations, irrigation frequency significantly affects the total water applied, with higher levels observed in I1 and I2 (50 % and 60 % soil moisture depletion) compared to the less frequent I4 and I5 treatments (80 % and 90 % depletion). The data reveal that elevated CO_2 (390 ppm) slightly reduces irrigation requirements across locations, suggesting improved water-use efficiency. Among the locations, Luxor and Al-Behera

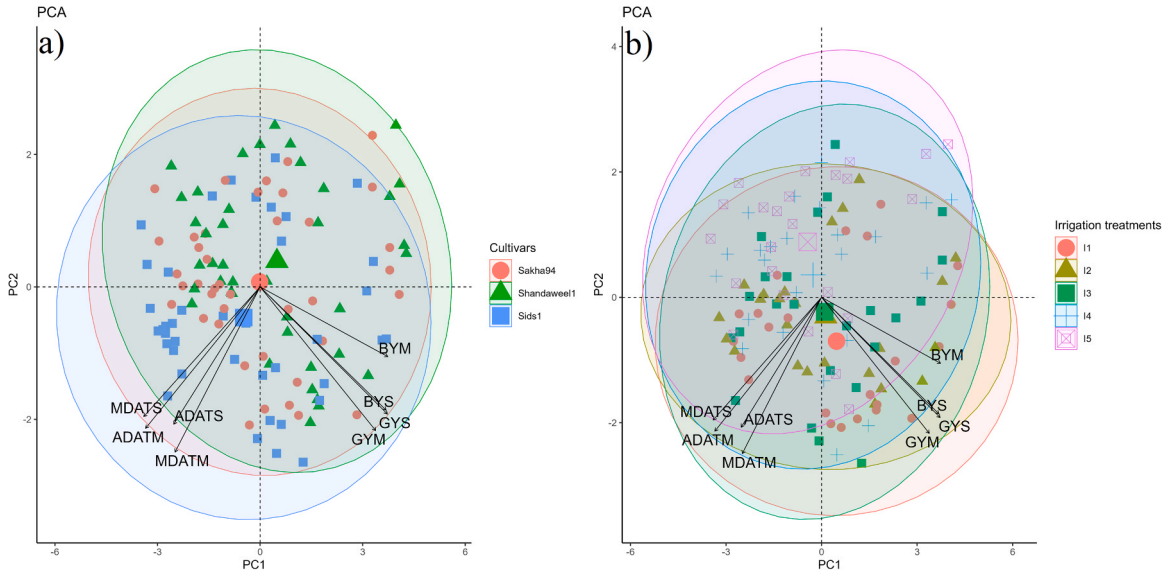

Fig. 6. Principal Component Analysis (PCA) illustrating the relationships among measured phenological and yield traits across three wheat cultivars (Sakha94, Shandweel1 and Sids1) and five irrigation treatments (I1–I5). Panel (a) shows the PCA distribution grouped by cultivar, highlighting the genetic influence of each cultivar on traits such as anthesis date (ADATS), maturity date (MDATS), grain yield (GYM), and biomass yield (BYM). Each cultivar exhibits unique clustering, with Shandweel1 displaying a wider spread along both principal components, suggesting a higher variability in response to environmental conditions and management practices. Panel (b) groups the PCA by irrigation treatments, emphasizing the effect of water availability on the variability of phenological and yield traits. Extreme irrigation treatments (I1 and I5) show broader dispersion along PC1, indicating greater variability in trait responses under these conditions, while moderate treatments (I2, I3, and I4) cluster more centrally, reflecting more stable responses. The PCA vectors indicate the alignment of phenological traits with PC1 and yield-related traits with PC2, underscoring the differential impact of genetic and irrigation factors on wheat performance. This analysis highlights the importance of cultivar selection and irrigation management in optimizing wheat productivity across diverse agro-climatic conditions.

generally required more irrigation than Al-Ismailia and Bani Suef, reflecting regional differences in environmental demands. This figure demonstrates the role of optimized irrigation scheduling and CO_2 levels in achieving efficient water use while maintaining yield across diverse agro-climatic conditions.

S. Fig. 4 presents water productivity (WP) based on evapotranspiration (ET), measured as kg/ha/mm, across different irrigation treatments, CO_2 level and locations for three wheat cultivars (Sakha94, Shandweel1 and Sids1) in Egypt. The figure demonstrates that WP generally improves with less frequent irrigation (I4 and I5), indicating higher water-use efficiency under greater water stress. Higher WP values are observed at 390 ppm CO_2 compared to 380 ppm, reflecting potential benefits of elevated CO_2 on water productivity. Among the locations, Luxor and Al-Behera typically exhibit higher WP compared to Al-Ismailia and Bani Suef, emphasizing the influence of environmental conditions. Overall, the results show the effectiveness of reduced irrigation regimes combined with elevated CO_2 in enhancing water productivity across diverse agro-climatic zones.

Fig. 8 presents chord diagrams showing the relationships between irrigation treatment and wheat cultivar for grain yield (panel a) and water productivity based on irrigation (panel b). In panel (a), the diagram reveals that grain yield is influenced by both the cultivar and the irrigation treatment, with Sakha94 and Shandweel1 displaying strong associations with higher irrigation levels (I1 and I2), indicating higher yield under frequent irrigation. Conversely, Sids1 shows relatively weaker connections across treatments, suggesting a more stable but moderate yield response across irrigation levels. Panel (b) illustrates water productivity based on irrigation, where stronger links are observed under lower irrigation frequencies (I4 and I5) for Shandweel1 and Sids1, indicating improved water-use efficiency under more restrictive irrigation regimes. Sakha94, while achieving high yields under frequent irrigation, shows lower water productivity under the same conditions, emphasizing the trade-off between yield maximization and water efficiency. These results highlight the cultivar-specific responses to irrigation levels, suggesting that Shandweel1 and Sids1 may be more suitable for water-limited environments due to their higher water productivity under deficit irrigation.

The mean relative changes in grain yield, water productivity based on evapotranspiration (WP_ET) and water productivity based on irrigation (WP_Irrigation) across various irrigation treatments (I2 to I5) relative to the no-stress treatment (I1, 50 % depletion) are presented in Fig. 9. The results indicate that grain yield generally declines as irrigation frequency decreases (from I2 to I5), with more pronounced reductions in locations such as Al-Behera and Al-Ismailia. Conversely, WP_Irrigation shows a marked increase under higher depletion levels, particularly under I5 (90 % depletion), suggesting that water-use efficiency improves as water availability becomes limited. This trend is especially evident in Al-Behera, where WP_Irrigation demonstrates substantial positive changes under I5, reflecting the ability of certain cultivars, such as Shandweel1, to maintain productivity under deficit irrigation. WP_ET al.so exhibits slight increases under reduced irrigation, indicating that crops use available water more efficiently when irrigation is limited. Overall, these findings suggest a trade-off between maximizing yield and improving water productivity, with reduced irrigation favoring water-use efficiency but impacting yield, particularly in more water-stressed environments.

The fixed and random effects of cultivar and irrigation treatment on grain yield (GY) and water productivity based on irrigation (WP_Irrigation) as estimated by a linear mixed model are presented (S. Fig. 5). The fixed effects (left panels) indicate significant differences in GY and WP_Irrigation across cultivars, with Sakha94 and Sids1 showing lower effect sizes compared to the intercept, suggesting cultivar-specific responses to water management strategies. The random effects (right panels) reveal that for GY, the largest deviations occur under lower soil moisture depletion levels (I1 and I2), which correspond to more frequent irrigation. In contrast, WP_Irrigation shows progressively higher random effects as irrigation frequency decreases (from I1 to I5), indicating improved water-use efficiency under greater water stress. These results suggest that while higher irrigation frequencies enhance grain yield, reduced irrigation levels improve WP_Irrigation, highlighting the

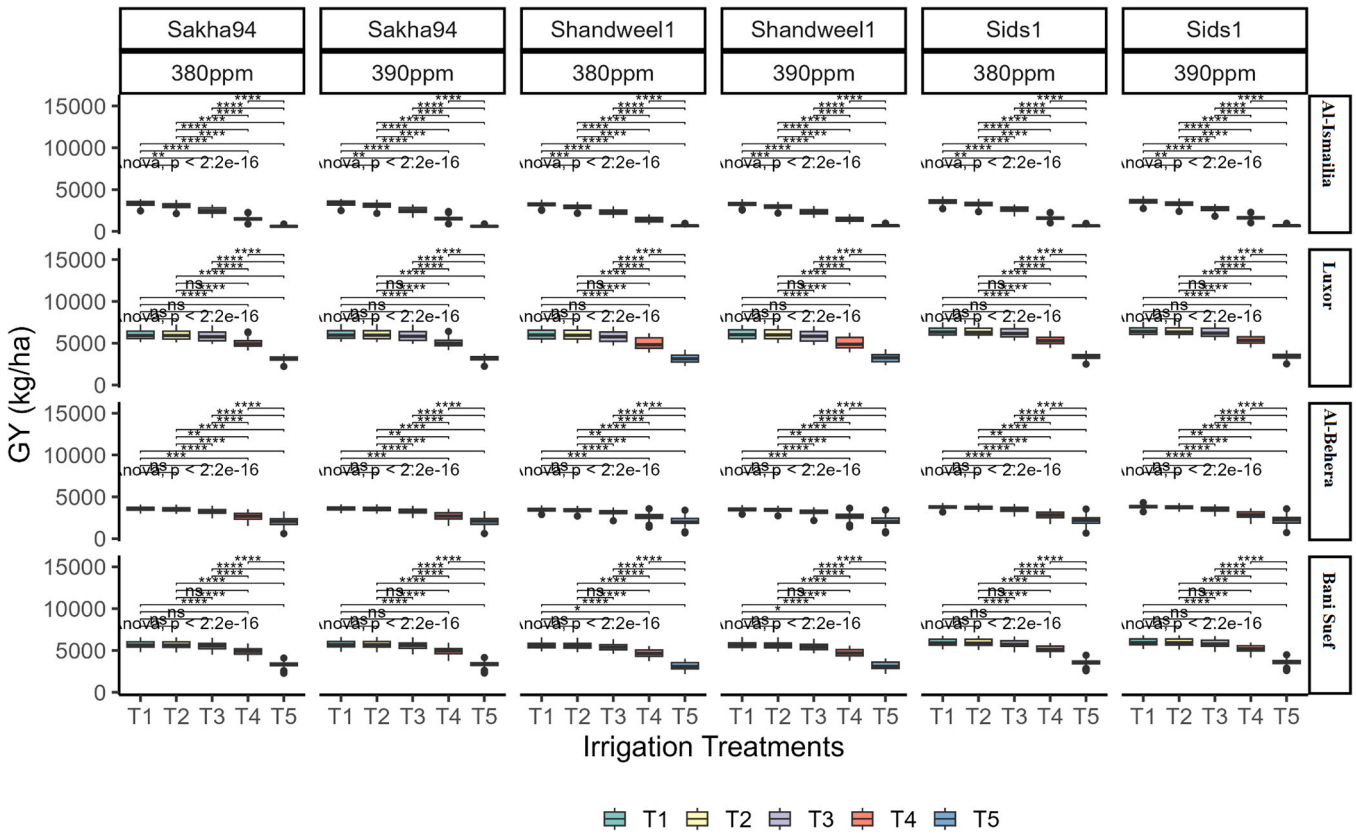

Fig. 7. Impact of irrigation treatment, CO_2 level and location on grain yield (GY) of different wheat cultivars (Sakha94, Shandweel1 and Sids1) in Egypt. This figure shows the response of grain yield (kg/ha) to five different irrigation treatments (I1 to I5) across four experimental sites— Al-Ismailia, Luxor, Al-Behera, and Bani Suef —under two CO_2 levels (380 ppm and 390 ppm) over 30 years of simulations (1981–2010). Each subplot represents a combination of cultivar and CO_2 level across locations, illustrating the variability in yield response due to interactions between irrigation frequency, cultivar type and environmental conditions. Statistical significance levels indicate differences between treatments, providing insights into optimal irrigation practices for each cultivar in varied agro-climatic zones. Irrigation treatments represent irrigation at 50 %, 60 %, 70 %, 80 % and 90 % depletion from soil available water for I1, I2, I3, I4 and I5 respectively.

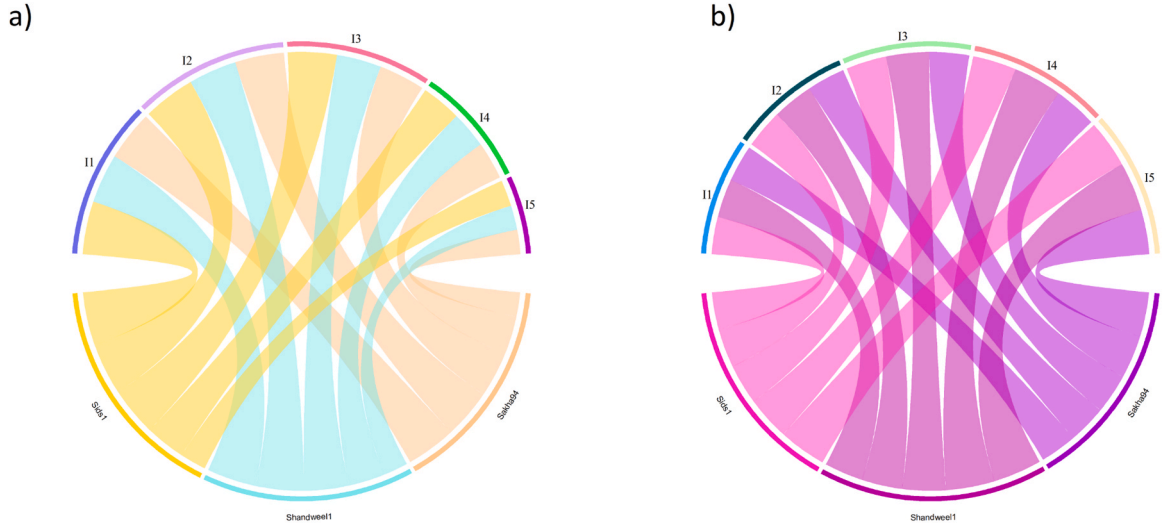

Fig. 8. Chord diagrams illustrating the relationships between irrigation treatment and wheat cultivar for (a) grain yield (kg/ha) and (b) water productivity based on irrigation (kg/ha/mm). In panel (a), the connections highlight the distribution of grain yield across five irrigation treatments (I1 to I5, representing 50 %, 60 %, 70 %, 80 % and 90 % soil moisture depletion) and three wheat cultivars (Sakha94, Shandweel1 and Sids1). Stronger links indicate higher yield performance under specific treatment-cultivar combinations. In panel (b), the links represent water productivity based on irrigation for each cultivar under the same irrigation treatments, showing how efficiently each cultivar uses water under varying moisture availability.

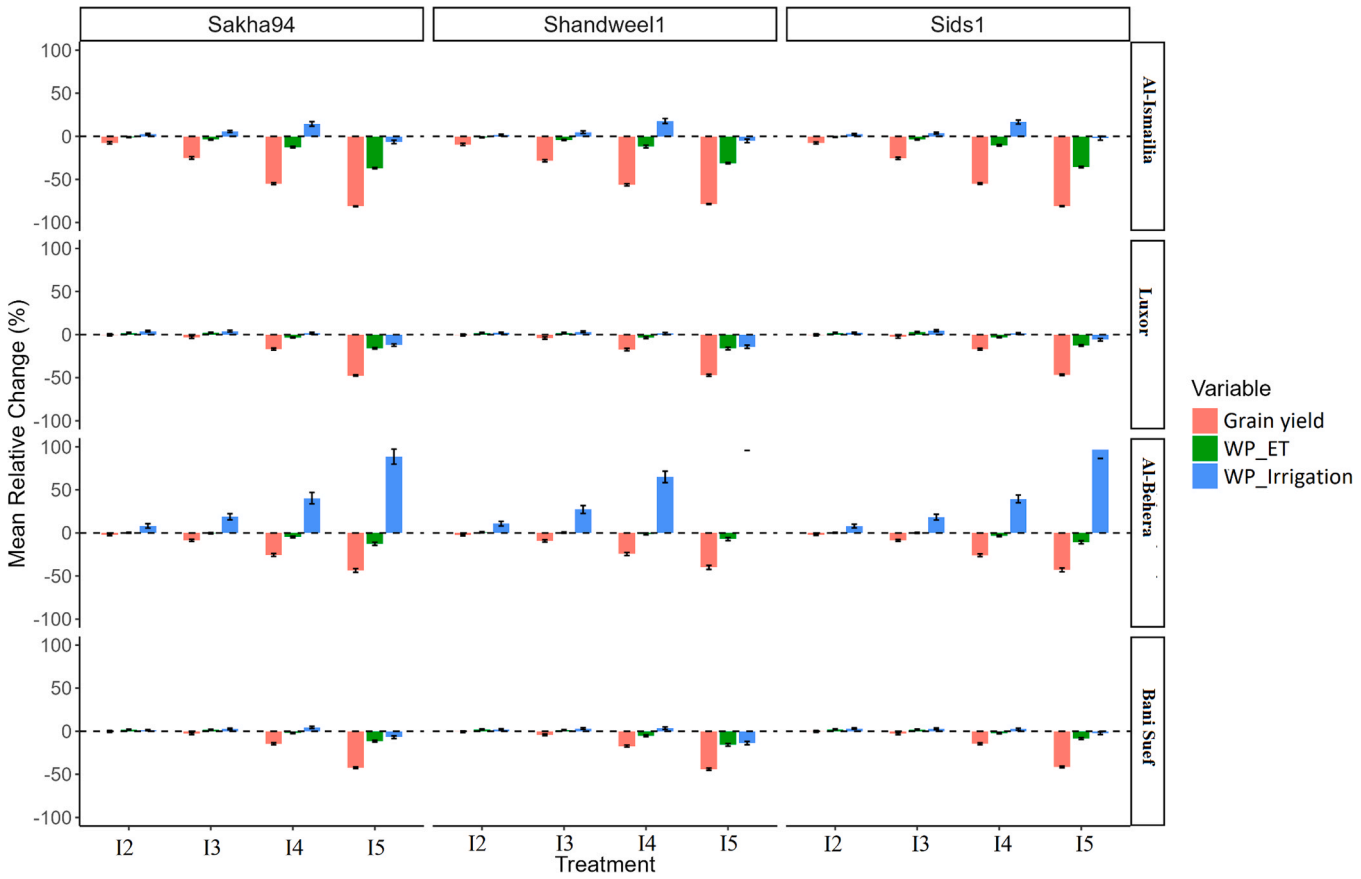

Fig. 9. Mean relative changes (%) in grain yield, water productivity based on evapotranspiration (WP_ET), and water productivity based on irrigation (WP_Irrigation) for three wheat cultivars (Sakha94, Shandweel1 and Sids1) across four locations (Al-Ismailia, Luxor, Al-Behera and Bani Suef) under different irrigation treatments (I2 to I5) relative to I1 (50 % depletion, no stress). Negative values indicate reductions, while positive values indicate increases compared to the no-stress baseline (I1). This figure highlights how reduced irrigation (I2 to I5) impacts yield and water productivity, with WP_Irrigation generally increasing under higher depletion levels (e.g., I5), especially in Al-Behera, indicating enhanced water-use efficiency under more restrictive irrigation regimes.

potential for optimizing both yield and water productivity by carefully balancing irrigation strategies across different cultivars.

3.3. Combination impacts of CO_2 and temperature on yield, and water productivity

The combined impacts of elevated CO_2 levels and temperature increases on wheat yield and water productivity were assessed across three cultivars, five irrigation treatments, and four locations. Results reveal distinct interactions between CO_2 enrichment, temperature increments, and management practices, as shown in Figs. 10 and 11 and Supplementary Figures S.6 and S.7. Fig. 10 illustrates that under moderate CO_2 levels (420–440 ppm) and a + 1°C temperature increment, grain yield improved by 10–20 % compared to baseline conditions (380 ppm CO_2 and +1°C) across all three cultivars under optimal irrigation (I1). For Sakha94, yields increased from 5.2 t/ha to 6.1 t/ha under these conditions. However, at + 3°C, yields dropped by up to 15 % for all cultivars under water-stressed conditions (I4 and I5). For instance, Giza168 under I5 showed a reduction from 3.8 t/ha (at +1°C) to 3.2 t/ha (at +3°C). These reductions emphasize the threshold effect of higher temperatures, with significant declines in yield observed beyond + 2°C. Fig. 11 quantifies the variability and percentage changes in grain yield. The upper panel highlights absolute yields across scenarios, showing peak yields of 6.4 t/ha under 440 ppm CO_2 and + 1°C, but reductions to as low as 2.8 t/ha under 380 ppm CO_2 and + 3°C for water-stressed treatments. The lower panel shows percentage changes, with yields increasing by up to 18 % under 420–460 ppm CO_2 at + 1°C, while declines of up to 25 % were observed under + 3°C scenarios, particularly for Sakha94 and Shandweel1 in water-limited conditions.

S. Fig. 6 highlights the impact of CO_2 and temperature on water productivity (kg/ha/mm ET). At 420 ppm CO_2 and + 1°C, WP increased by 15–25 % across all cultivars and irrigation treatments, with maximum gains observed under deficit irrigation (I4 and I5). For example, Shandweel1 under I5 showed an improvement from 12 kg/ha/mm ET at baseline to 15.3 kg/ha/mm ET. However, WP gains were marginal under + 3°C, with reductions of up to 12 % observed at lower CO_2 levels (380–400 ppm). Sakha94 exhibited the least improvement in WP under water-stressed conditions at + 3°C, highlighting its sensitivity to combined heat and water stress. S. Fig. 7 shows that elevated temperatures shortened the wheat growth cycle across all cultivars, with growth durations decreasing by 8–14 days under + 2°C and up to 20 days under + 3°C. For instance, the growth cycle for Giza168 decreased from 135 days at baseline to 115 days under + 3°C. Shortened growth periods limited the grain-filling phase, reducing yield potential despite CO_2 enrichment. This effect was more pronounced in water-stressed treatments (I4 and I5) and for heat-sensitive cultivars like Sakha94.

Quantitatively, the results emphasize that moderate CO_2 enrichment (420–440 ppm) can enhance yield by up to 20 % and WP by 25 % under + 1°C to + 2°C scenarios, particularly for water-efficient cultivars like Giza168. However, at + 3°C, these benefits diminish, with yield reductions of up to 25 % and WP losses of 12 % under stressed conditions. These findings underscore the critical need for targeted cultivar selection and irrigation management to mitigate the impacts of rising temperatures and optimize the benefits of CO_2 enrichment in wheat production.

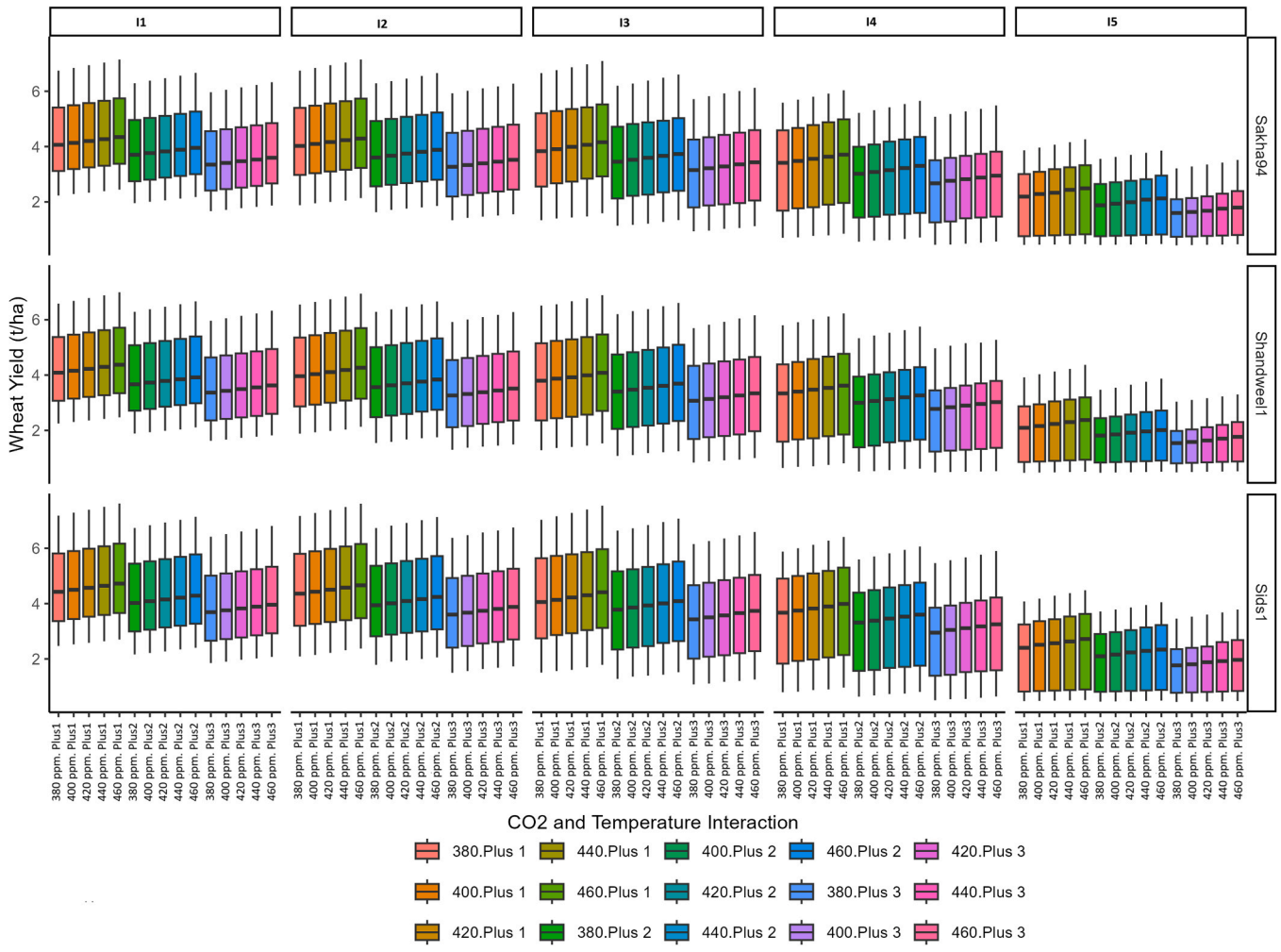

Fig. 10. Impact of CO_2 concentration and temperature increases on wheat yield across different cultivars and irrigation treatments.
This figure illustrates the combined effects of varying CO_2 levels and temperature increases on the wheat yield for multiple cultivars ('Sakha94', 'Shandweel1', and 'Giza168') under five different irrigation treatments (I1 to I5). Each boxplot represents the distribution of wheat yield outcomes under specific combinations of CO_2 concentration (ranging from 380 ppm to 460 ppm) and temperature scenarios (labeled as 'Plus 1′, 'Plus 2′, 'Plus 3′, indicating incremental temperature increases with +1, +2, and +3 C above baseline). The variability within each category highlights the sensitivity of wheat yield to these climatic factors, showcasing the differential adaptive capacity of each cultivar and irrigation strategy.

4. Discussion

The calibration results revealed moderate model performance for simulating phenological stages (anthesis and maturity), with acceptable d-index levels (~0.6), indicating partial agreement with observed trends across diverse environments. In contrast, predictions for grain and biomass yields were more accurate, as reflected by higher d-index values (0.76–0.81), demonstrating the model's strength in capturing yield variability under different irrigation treatments. The lower phenological precision is likely due to the combined effects of site-specific climate variability and cultivar-specific responses to water stress, which are not fully captured by standard calibration. This is may be due to the unrealistic water stress parameterization which strongly affected the GLUE algorithm in locating calibrated parameters (Yan et al., 2020). These findings highlight the complexity of simulating phenology under variable field conditions and suggest that further refinement—such as incorporating advanced calibration techniques and adopting multi-model ensemble approaches—may improve model robustness for scenario-based applications.

Consequently, adopting more robust calibration approaches—particularly multi-approaches ensemble techniques (Jha et al., 2022)—represents a promising direction for improving phenology simulations under stress conditions. One of the most advanced frameworks is the calibration methodology developed under Phase 3 of the Agricultural Model Intercomparison and Improvement Project (AgMIP) (Rosenzweig et al., 2013), which includes the use of CroptimizR (Buis et al., 2023) and CroPlotR (Vezy et al., 2023) packages. Integrated within the DSSAT-wrapper, these tools offer a flexible and efficient calibration system capable of handling multiple experimental files, treatments, and various types of observational data. However, this approach requires detailed input, including end-of-season and time-series observations, which can be complemented by remote sensing data assimilation (Niu et al., 2021; Pasquel et al., 2022) to enhance calibration accuracy and temporal resolution.

This study addresses two of the most impactful challenges faced by developing countries today: food security (Finger, 2011; Godfray et al., 2010) and water security (Vörösmarty et al., 2010), both of which are under significant strain due to limited resources and growing climate variability. As wheat is a staple crop critical to food security in many arid and semi-arid regions, optimizing its production under water-limited conditions is essential for sustaining livelihoods and reducing vulnerability to resource shortages. The discussion highlights the critical findings of this study on the effects of irrigation treatments and elevated CO_2 level on wheat yield, evapotranspiration (ET) and water productivity

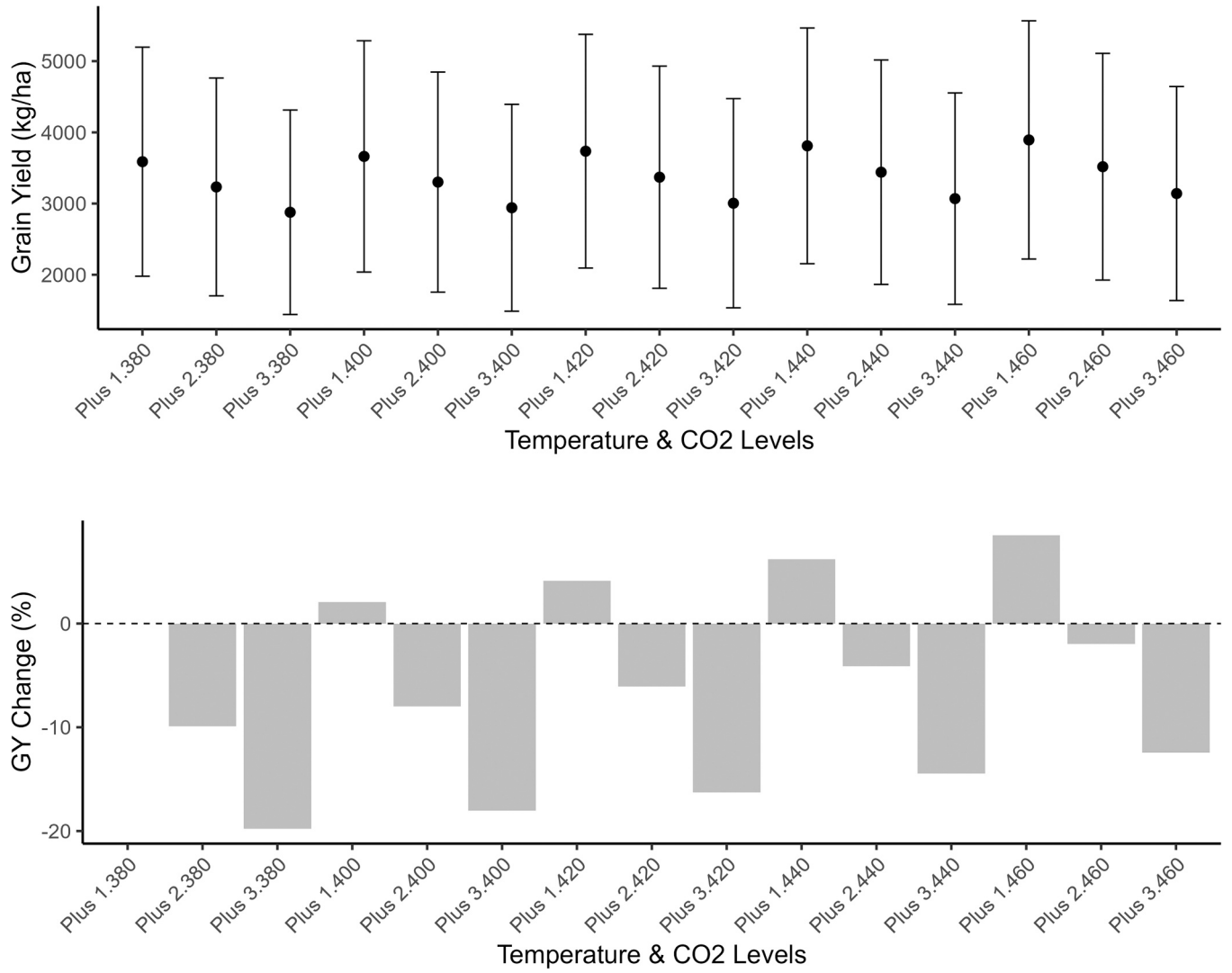

Fig. 11. Variability and relative change in grain yield under different temperature and CO_2 scenarios.
The upper panel displays the grain yield (kg/ha) variability across a range of combined temperature and CO_2 level scenarios, denoted as 'Plus X_YYY', where 'X' indicates the temperature increase (+1 °C, +2 °C, and +3 °C) and 'YYY' the CO_2 concentration in ppm (380 ppm, 400 ppm, 420 ppm, 440 ppm and 460 ppm). The error bars represent the range of yield outcomes observed. The lower panel quantifies the percentage change in grain yield relative to the reference condition of 'Plus 1 °C and 380 ppm', where a temperature increment of 'Plus 1' and a CO_2 level of 380 ppm serve as the reference point. Each bar in the lower panel reflects the relative change compared to this baseline, with the dotted line at 0 % illustrating no change from the baseline. This dual visualization effectively demonstrates both the absolute yield values and their relative fluctuations due to incremental increases in temperature and CO_2 levels.

(WP) across diverse agro-climatic zones in Egypt. The results reveal that higher irrigation frequencies (I1 and I2) generally lead to increased grain yields, with significant yield responses observed in the cultivar Sakha94 under both current (380 ppm) and elevated CO_2 levels (390 ppm). This finding aligns with previous studies indicating that frequent irrigation enhances crop productivity in arid and semi-arid regions by maintaining optimal soil moisture conditions for growth (Ali et al., 2020; Asseng et al., 2018). However, this study also demonstrates that when irrigation frequency is reduced (I4 and I5), WP, particularly WP_Irrigation, increases markedly, suggesting enhanced water-use efficiency under deficit irrigation conditions (Kheir et al., 2021; Leghari et al., 2024; Wakchaure et al., 2020). This response is particularly prominent in the cultivars Shandweel1 and Sids1, indicating their adaptability to water-limited environments—a finding consistent with past research on cultivar-specific responses to deficit irrigation (Ding et al., 2021; Kheir et al., 2022).

The influence of elevated CO_2 on both yield and WP is notable. This study found that 390 ppm CO_2 slightly improved yield and reduced ET across all treatments, suggesting potential future benefits in a high-CO_2 environment. Similar findings from Asseng et al. (2018) and (Zhang et al., 2021), stated that elevated CO_2 enhances photosynthetic efficiency and reduces transpiration, thus increasing water-use efficiency. However, this effect was more pronounced in locations with higher yield potential (e.g., Al-Behera and Luxor), suggesting that CO_2 enrichment may interact positively with high-yield environments, a result corroborated by Ali et al. (2020) who reported greater CO_2-induced yield gains in fertile regions in Egypt. This outcome underscores the potential for elevated CO_2 to support yield improvements, albeit with site-specific variability in effectiveness.

The linear mixed model analysis provides further insights into the fixed and random effects of cultivar and irrigation treatment on GY and WP_Irrigation. The fixed effects indicate that cultivars respond differently to irrigation, with Sakha94 benefiting more from frequent irrigation in terms of yield, while Shandweel1 and Sids1 show better WP_Irrigation under reduced irrigation. The random effects suggest that WP_Irrigation increases with higher depletion levels, which highlights the effectiveness of water-saving strategies in boosting water productivity, especially in water-scarce regions. These findings offer a balanced

understanding of how different irrigation regimes and cultivars interact to influence both yield and water productivity, providing a plan for optimizing wheat production in arid zones where water conservation is essential.

Compared to past studies (Grant et al., 1999; Pazzagli et al., 2016), this research contributes unique insights into cultivar-specific responses to irrigation and CO_2 interactions in Egypt's agro-climatic zones, addressing an important knowledge gap. The use of DSSAT modeling, coupled with field data, enhances the credibility of these findings by providing robust predictions under variable conditions. However, limitations exist, particularly concerning the model's reliance on calibration data from specific locations, which may not fully explain the diversity of Egypt's micro-climates. Moreover, the DSSAT model's single-crop focus limits its applicability for analyzing crop rotations or intercropping systems, which are increasingly relevant in water-limited regions (Hernández-Ochoa et al., 2022).

To address these limitations and improve predictive robustness, future research should incorporate a multi-model ensemble approach (Martre et al., 2015), drawing from models like APSIM (Kheir et al., 2023; Ren et al., 2024) and AquaCrop (Adla et al., 2024), alongside DSSAT. A multi-model ensemble would allow for cross-validation of results and provide a more comprehensive understanding of model uncertainties (Jamatutu et al., 2024). Quantifying these uncertainties is essential to provide reliable recommendations for farmers and policymakers. Furthermore, future studies should explore the impacts of recent climate scenarios, particularly those from CMIP6 (Sa'adi et al., 2024; Zhu et al., 2023), which offer more refined projections on temperature, precipitation and CO_2 concentration. By examining these scenarios, researchers can assess the future impacts of climate change on wheat production in Egypt, including potential risks to yield stability and water resources under various warming trajectories.

The results of the sensitivity analysis demonstrate the complex interplay between CO_2 enrichment and temperature increases on wheat growth and productivity, emphasizing the importance of cultivar and irrigation management in adapting to future climate scenarios. Elevated CO_2 concentrations consistently showed positive effects by enhancing photosynthesis and reducing stomatal conductance, which improved water productivity and partially offset the negative impacts of higher temperatures (AINSWORTH and ROGERS, 2007). However, as illustrated in S. Fig. 7, higher temperatures (+2°C and +3°C) significantly shortened the wheat growth period across all cultivars, reducing the grain-filling phase and ultimately limiting the yield benefits from CO_2 enrichment. For example, the growth cycle for Giza168 decreased by up to 20 days under + 3°C, highlighting the temperature sensitivity of phenological development.

Deficit irrigation treatments (I4 and I5) further exacerbated the challenges posed by higher temperatures, as reduced water availability intensified the stress during critical growth stages. While elevated CO_2 levels enhanced water productivity under these conditions, the yield gains were less pronounced for heat-sensitive cultivars like Sakha94 compared to the more resilient Giza168. This suggests that CO_2-induced water use efficiency improvements may not fully mitigate the combined effects of heat and water stress, particularly for cultivars with shorter grain-filling periods or higher temperature sensitivity (Asseng et al., 2015). Nonetheless, the combined effects of moderate CO_2 enrichment (420–440 ppm) and mild temperature increases (+1°C to +2°C) under deficit irrigation showed some promise for sustaining yields in water-scarce environments, particularly for cultivars like Shandweel1 that exhibit greater adaptability.

These findings underscore the need for climate-resilient strategies that integrate cultivar selection and irrigation optimization. Breeding programs should focus on developing cultivars with longer grain-filling periods and enhanced heat tolerance to maximize the synergistic benefits of CO_2 enrichment. Additionally, irrigation scheduling must be tailored to mitigate heat stress during critical phenological stages, especially under deficit irrigation systems. These results align with previous studies suggesting that elevated CO_2 can buffer some adverse impacts of climate change but requires a systems-level approach to achieve sustainable agricultural productivity (Cui et al., 2024; Lobell et al., 2011).

Finally, expanding the scope of research to include sensitivity analyses of other environmental and management factors (e.g., soil types, pest pressures, nutrient availability) would enhance the applicability of model outputs and support more resilient agricultural planning. Additionally, we recommend future studies adopt a multi-model ensemble approach (Wallach et al., 2018) to cross-validate findings and expand field experiments to capture broader environmental variability. These steps enhance the robustness of our results, providing more reliable recommendations for optimizing wheat production under diverse conditions. To ensure the practical application of the model outputs for farmers, delivery mechanisms tailored to local circumstances are crucial. Mobile-based solutions, including text messaging and applications managed by the Agricultural Extension Services or the Ministry of Agriculture, can bridge the gap between research findings and on-ground implementation, ensuring accessibility even in regions with limited internet connectivity.

5. Conclusion

This study emphasizes the importance of targeted irrigation management and cultivar selection for improving wheat productivity and water-use efficiency in arid regions. Using the DSSAT CERES-Wheat model integrated with field data, the findings show that frequent irrigation maximizes yield in cultivars like Sakha94, while deficit irrigation enhances water productivity, particularly in Shandweel1 and Sids1. Elevated CO_2 levels (420–440 ppm) positively impact yield and water productivity, especially under mild temperature increases (+1°C to +2°C). However, higher temperatures (+3°C) shortened the growth cycle, limiting the benefits of CO_2 and reducing yield, particularly in heat-sensitive cultivars like Sakha94.

The sensitivity analysis underscores the need for location-specific strategies that combine climate-resilient cultivars and optimized irrigation practices to mitigate water scarcity and heat stress. Future research should expand on these findings by integrating multi-model ensembles, exploring CMIP6 climate scenarios, and addressing additional factors like soil health and pest control. This study provides valuable insights for developing resilient agricultural systems in Egypt and other water-scarce regions, balancing productivity with resource conservation.

CRediT authorship contribution statement

Maha L. Elsayed: Writing – review & editing, Project administration, Formal analysis, Conceptualization, Writing – original draft, Funding acquisition, Data curation. **Ahmed F. Elkot:** Methodology, Data curation. **Tahany Noreldin:** Investigation, Formal analysis. **Benjamin Richard:** Methodology, Formal analysis, Writing – review & editing, Investigation, Data curation. **Aiming Qi:** Investigation, Data curation, Writing – review & editing, Formal analysis. **Yasser M. Shabana:** Writing – original draft, Conceptualization, Writing – review & editing, Resources. **Samir M. Saleh:** Formal analysis, Investigation. **Bruce D.L. Fitt:** Writing – review & editing, Investigation, Data curation, Methodology, Formal analysis. **Ahmed M.S. Kheir:** Writing – review & editing, Visualization, Formal analysis, Writing – original draft, Supervision, Conceptualization.

Funding

This research was supported by research grants from funds Science, Technology and Innovation Funding Authority (STDF) (grant number [42687" EG - US cycle 19] and Newton Fund Impact Scheme funds by the British Council and STDF (Project ID: 43937).

Declaration of Competing Interest

The authors declare no conflicts of interest

Acknowledgments

We are grateful to research funders Egyptian Science, Technology and Innovation Funding Authority (STDF) grant number 42687" EG - US cycle 19. We are also grateful to Newton Fund Impact Scheme funds by British Council - STDF Project ID: 43937. We gratefully acknowledge help in running the irrigation experiments by Wheat Research Department, Field Crops Research Institute, Agricultural Research Center, and Agricultural Research Stations at Al-Ismailia, Luxor, Al-Behera, and Bani Suef. Authors would like also to thank Dr. Alaa Hamwieh, ICARDA, Egypt for advice and recommendations.

Appendix A. Supporting information

Supplementary data associated with this article can be found in the online version at doi:10.1016/j.agwat.2025.109668.

Data availability

Data will be made available on request.

References

Abdalla, A., Stellmacher, T., Becker, M., 2023. Trends and Prospects of Change in Wheat Self-Sufficiency in Egypt. Agriculture 13 (1), 7.
Abdelhafez, A.A., Metwalley, S.M., Abbas, H.H., 2020. Irrigation: Water Resources, Types and Common Problems in Egypt. In: Omran, E.-S.E., Negm, A.M. (Eds.), Technological and Modern Irrigation Environment in Egypt: Best Management Practices & Evaluation. Springer International Publishing, Cham, pp. 15–34.
Abdelmageed, K., et al., 2019. Evolution of varieties and development of production technology in Egypt wheat: A review. J. Integr. Agric. 18 (3), 483–495.
Abou-Hadid, A.F., 2025. Impact of Climate Change on Egyptian Agriculture, Challenges, and Opportunities. In: Khalil, M.T., Emam, W.W.M., Negm, A. (Eds.), Climate Changes Impacts on Aquatic Environment: Assessment, Adaptation, Mitigation, and Road Map for Sustainable Development. Springer Nature Switzerland, Cham, pp. 171–182.
Adla, S., et al., 2024. Impact of calibrating a low-cost capacitance-based soil moisture sensor on AquaCrop model performance. J. Environ. Manag. 353, 120248.
AINSWORTH, E.A., ROGERS, A., 2007. The response of photosynthesis and stomatal conductance to rising [CO2]: mechanisms and environmental interactions. Plant Cell Environ. 30 (3), 258–270.
Ali, M.G.M., et al., 2020. Climate change impact and adaptation on wheat yield, water use and water use efficiency at North Nile Delta. Front. Earth Sci. 14 (3), 522–536.
Ammar, K.A., Kheir, A.M.S., Ali, B.M., Sundarakani, B., Manikas, I., 2024. Developing an analytical framework for estimating food security indicators in the United Arab Emirates: a review. Environ. Dev. Sustain. 26 (3), 5689–5708.
Asseng, S., et al., 2015. Rising temperatures reduce global wheat production. Nat. Clim. Change 5 (2), 143–147.
Asseng, S., et al., 2018. Can Egypt become self-sufficient in wheat? Environ. Res. Lett. 13 (9), 094012.
Buis, S., Lecharpentier, P., Vezy, R. and Ginet, M., 2023. CroptimizR: a package to estimate parameters of crop models [WWW Document]. In: h.d.o.z. 4066451. (Editor).
Cheng, C.L., Shalabh, Garg, G., 2014. Coefficient of determination for multiple measurement error models. J. Multivar. Anal. 126, 137–152.
Chiarelli, D.D., et al., 2022. Competition for water induced by transnational land acquisitions for agriculture. Nat. Commun. 13 (1), 505.
Cookson-Hills, C., 2008. Irrigation in Egypt. In: Selin, H. (Ed.), Encyclopaedia of the History of Science, Technology, and Medicine in Non-Western Cultures. Springer Netherlands, Dordrecht, pp. 1–4.
Cui, J., et al., 2024. Elevated CO2 levels promote both carbon and nitrogen cycling in global forests. Nat. Clim. Change 14 (5), 511–517.
Ding, Z., et al., 2021. Modeling the combined impacts of deficit irrigation, rising temperature and compost application on wheat yield and water productivity. Agric. Water Manag. 244, 106626.
Elkot, A.F., et al., 2024. Yield Responses to total water input from irrigation and rainfall in six wheat cultivars under different climatic zones in Egypt. Agronomy 14 (12), 3057.
Elsadek, E.A., et al., 2024. Impacts of climate change on rice yields in the Nile River Delta of Egypt: A large-scale projection analysis based on CMIP6. Agric. Water Manag. 292, 108673.
Elsayed, M., et al., 2017. Assessment of transplanting date influence on processing tomato (Lycopersicon esculentum Mill.) production using the cropping system model (CSM)-CROPGRO-tomato simulation model a case study for northeastern Italy. Egypt. J. Soil Sci. 57 (4), 429–442.
Elsayed, M., Medany, M., Hoogenboom, G., Bona, S., Sambo, P., 2012. EVALUATION OF THE DSSAT CSM-CROPGRO-TOMATO SIMULATION MODEL FOR PROCESSING TOMATO (LYCOPERSICON ESCULENTUM MILL.) PRODUCTION IN NORTHERN ITALY. International Society for Horticultural Science (ISHS), Leuven, Belgium, pp. 423–428.
Falconnier, G.N., et al., 2020. Modelling climate change impacts on maize yields under low nitrogen input conditions in sub-Saharan Africa. Glob. Change Biol. 26 (10), 5942–5964.
Fang, Y., et al., 2024. Assessing the impact of early and terminal droughts on root growth, grain yield and yield stability in old and modern wheat cultivars on the Loess Plateau. Agric. Water Manag. 301, 108940.
Finger, R., 2011. Food security: Close crop yield gap. Nature 480 (7375), 39. -39.
Gebeltová, Z., et al., 2023. Geopolitical risks for Egypt wheat supply and trade. Front. Sustain. Food Syst. 7.
Geerts, S., Raes, D., 2009. Deficit irrigation as an on-farm strategy to maximize crop water productivity in dry areas. Agric. Water Manag. 96 (9), 1275–1284.
Godfray, H.C.J., et al., 2010. Food security: the challenge of feeding 9 billion people. Science 327 (5967), 812–818.
Grant, R.F., et al., 1999. Crop water relations under different CO2 and irrigation: testing of ecosys with the free air CO2 enrichment (FACE) experiment. Agric. For. Meteorol. 95 (1), 27–51.
Han, J.-C., Huang, G.-H., Zhang, H., Li, Z., Li, Y.-P., 2014. Bayesian uncertainty analysis in hydrological modeling associated with watershed subdivision level: a case study of SLURP model applied to the Xiangxi River watershed, China. Stoch. Environ. Res. Risk Assess. 28 (4), 973–989.
Hernández-Ochoa, I.M., et al., 2022. Model-based design of crop diversification through new field arrangements in spatially heterogeneous landscapes. A review. Agron. Sustain. Dev. 42 (4), 74.
Ingrao, C., Strippoli, R., Lagioia, G., Huisingh, D., 2023. Water scarcity in agriculture: An overview of causes, impacts and approaches for reducing the risks. Heliyon 9 (8), e18507.
Jacovides, C.P., Kontoyiannis, H., 1995. Statistical procedures for the evaluation of evapotranspiration computing models. Agric. Water Manag. 27 (3), 365–371.
Jamatutu, S.A., et al., 2024. Quantifying future carbon emissions uncertainties under stochastic modeling and Monte Carlo simulation: insights for environmental policy consideration for the Belt and Road Initiative Region. J. Environ. Manag. 370, 122463.
Janssen, P.H.M., Heuberger, P.S.C., 1995. Calibration of process-oriented models. Ecol. Model. 83 (1), 55–66.
Jha, P.K., Ines, A.V.M., Han, E., Cruz, R., Vara Prasad, P.V., 2022. A comparison of multiple calibration and ensembling methods for estimating genetic coefficients of CERES-Rice to simulate phenology and yields. Field Crops Res. 284, 108560.
Jones, J.W., et al., 2003. The DSSAT cropping system model. Eur. J. Agron. 18 (3), 235–265.
Jones, J.W., et al., 2011. Estimating DSSAT cropping system cultivar-specific parameters using bayesian techniques. Methods Introd. Syst. Models into Agric. Res. 365–393.
Karimi, M., Tabiee, M., Karami, S., Karimi, V., Karamidehkordi, E., 2024. Climate change and water scarcity impacts on sustainability in semi-arid areas: lessons from the South of Iran. Groundw. Sustain. Dev. 24, 101075.
Kheir, A.M.S., et al., 2019. Impacts of rising temperature, carbon dioxide concentration and sea level on wheat production in North Nile delta. Sci. Total Environ. 651, 3161–3173.
Kheir, A.M.S., et al., 2020b. Wheat Crop Modelling for Higher Production. In: Ahmed, M. (Ed.), Systems Modeling. Springer, Singapore, Singapore, pp. 179–202.
Kheir, A.M.S., et al., 2021. Modeling deficit irrigation-based evapotranspiration optimizes wheat yield and water productivity in arid regions. Agric. Water Manag. 256, 107122.
Kheir, A.M.S., et al., 2022a. Cereal Crop Modeling for Food and Nutrition Security. In: Ahmed, M. (Ed.), Global Agricultural Production: Resilience to Climate Change. Springer International Publishing, Cham, pp. 183–195.
Kheir, A.M.S., et al., 2022b. Minimizing trade-offs between wheat yield and resource-use efficiency in the Nile Delta – a multi-model analysis. Field Crops Res. 287, 108638.
Kheir, A.M.S., et al., 2023. Integrating APSIM model with machine learning to predict wheat yield spatial distribution. Agron. J. 115 (6), 3188–3196.
Kheir, A.M.S., et al., 2024. Impacts of climate change on spatial wheat yield and nutritional values using hybrid machine learning. Environ. Res. Lett. 19 (10), 104049.
Kheir, A.M.S., et al., 2025. Hybridization of process-based models, remote sensing, and machine learning for enhanced spatial predictions of wheat yield and quality. Comput. Electron. Agric. 234, 110317.
Kheir, A.M.S., Abdelaal, A.I.N., Hoogenboom, G. and Asseng, S., 2020a. Experimental and simulated wheat data from across a temperature gradient along the River Nile in Egypt. Open Data Journal for Agricultural Research, 6(⟨https://odjar.org/article/view/16318/17326⟩): 19-20.
Leghari, S.J., et al., 2024. What should we do for water security? A technical review on more yield per water drop. J. Environ. Manag. 370, 122832.
Li, L., Xia, J., Xu, C.-Y., Singh, V.P., 2010. Evaluation of the subjective factors of the GLUE method and comparison with the formal Bayesian method in uncertainty assessment of hydrological models. J. Hydrol. 390 (3), 210–221.
Lobell, D.B., Schlenker, W., Costa-Roberts, J., 2011. Climate trends and global crop production since 1980. Science 333 (6042), 616–620.
Martre, P., et al., 2015. Multimodel ensembles of wheat growth: many models are better than one. Glob. Change Biol. 21 (2), 911–925.

McCown, R.L., Hammer, G.L., Hargreaves, J.N.G., Holzworth, D.P., Freebairn, D.M., 1996. APSIM: a novel software system for model development, model testing and simulation in agricultural systems research. Agric. Syst. 50 (3), 255–271.
Niu, Z., et al., 2021. A Process-Based Model Integrating Remote Sensing Data for Evaluating Ecosystem Services. J. Adv. Model. Earth Syst. 13 (6), e2020MS002451.
Pasley, H., et al., 2023. APSIM next generation mungbean model: A tool for advancing mungbean production. Field Crops Res. 298, 108955.
Pasquel, D., et al., 2022. A review of methods to evaluate crop model performance at multiple and changing spatial scales. Precis. Agric. 23 (4), 1489–1513.
Pathria, R.K., Beale, P.D., 2011. 1 - The Statistical Basis of Thermodynamics. In: Pathria, R.K., Beale, P.D. (Eds.), Statistical Mechanics, Third Edition. Academic Press, Boston, pp. 1–23.
Pazzagli, P.T., Weiner, J., Liu, F., 2016. Effects of CO2 elevation and irrigation regimes on leaf gas exchange, plant water relations, and water use efficiency of two tomato cultivars. Agric. Water Manag. 169, 26–33.
R Core Team, 2024. R: A language and environment for statistical computing. R Foundation for Statistical Computing, Vienna, Austria.
Ren, W., et al., 2024. Evaluating nitrogen dynamic and utilization under controlled-release fertilizer application for sunflowers in an arid region: Experimental and modeling approach. J. Environ. Manag. 370, 122456.
Rosenzweig, C., et al., 2013. The agricultural model intercomparison and improvement project (AgMIP): protocols and pilot studies. Agric. For. Meteorol. 170, 166–182.
Ruane, A.C., Goldberg, R., Chryssanthacopoulos, J., 2015. Climate forcing datasets for agricultural modeling: Merged products for gap-filling and historical climate series estimation. Agric. For. Meteorol. 200, 233–248.
Sa'adi, Z., et al., 2024. Observed and future shifts in climate zone of Borneo based on CMIP6 models. J. Environ. Manag. 360, 121087.
Solgi, S., Ahmadi, S.H., Sepaskhah, A.R., Edalat, M., 2022. Wheat yield modeling under water-saving irrigation and climatic scenarios in transition from surface to sprinkler irrigation systems. J. Hydrol. 612, 128053.
Vezy, R., Buis, S., Lecharpentier, P., Giner, M., 2023. In: h.d.o.z.W. Document]. (Editor). Crop. A Package Anal. Crop.Model Simul. Outputs Plots Stat.
Vörösmarty, C.J., et al., 2010. Erratum: Global threats to human water security and river biodiversity. Nature 468 (7321), 334. -334.
Wakchaure, G.C., Minhas, P.S., Meena, K.K., Kumar, S., Rane, J., 2020. Effect of plant growth regulators and deficit irrigation on canopy traits, yield, water productivity and fruit quality of eggplant (Solanum melongena L.) grown in the water scarce environment. J. Environ. Manag. 262, 110320.
Wallach, D., et al., 2018. Multimodel ensembles improve predictions of crop–environment–management interactions. Glob. Change Biol. 24 (11), 5072–5083.
Wu, P., et al., 2024. Evaluating optimized irrigation strategies on crop productivity and field water utilization under micro sprinkling irrigation in typical cropping systems of the Huang-Huai-Hai Plain. Eur. J. Agron. 154, 127093.
Yan, L., Jin, J., Wu, P., 2020. Impact of parameter uncertainty and water stress parameterization on wheat growth simulations using CERES-Wheat with GLUE. Agric. Syst. 181, 102823.
Zhang, Y., Niu, H., Yu, Q., 2021. Impacts of climate change and increasing carbon dioxide levels on yield changes of major crops in suitable planting areas in China by the 2050s. Ecol. Indic. 125, 107588.
Zhu, Q., et al., 2023. Modeling soybean cultivation suitability in China and its future trends in climate change scenarios. J. Environ. Manag. 345, 118934.
Ziaei, A.N., Sepaskhah, A.R., 2003. Model for simulation of winter wheat yield under dryland and irrigated conditions. Agric. Water Manag. 58 (1), 1–17.